Korpi, Antti; Anaya-Plaza, Eduardo; Välimäki, Salla; Kostiainen, Mauri

Highly ordered protein cage assemblies

Published in:
Wiley Interdisciplinary Reviews: Nanomedicine and Nanobiotechnology

DOI:
10.1002/wnan.1578

Published: 01/01/2019

Document Version
Peer-reviewed accepted author manuscript, also known as Final accepted manuscript or Post-print

Highly ordered protein cage assemblies: a toolkit for new materials

First author Antti Korpi‡, Biohybrid Materials, Department of Bioproducts and Biosystems, Aalto University, 00076 Aalto, Finland antti.korpi@aalto.fi
Second author Eduardo Anaya-Plaza‡, 0000-0001-9944-6907, Biohybrid Materials, Department of Bioproducts and Biosystems, Aalto University, 00076 Aalto, Finland. eduardo.anaya@aalto.fi
Third author Salla Välimäki, Biohybrid Materials, Department of Bioproducts and Biosystems, Aalto University, 00076 Aalto, Finland salla.valimaki@aalto.fi
Fourth author Mauri Kostiainen*, 0000-0002-8282-2379, Biohybrid Materials, Department of Bioproducts and Biosystems, Aalto University, 00076 Aalto, Finland mauri.kostiainen@aalto.fi

‡ The authors contributed equally to this paper.

Abstract

Protein capsids are specialized and versatile natural macromolecules with exceptional properties. Their homogenous, spherical, rod-like or toroidal geometry, and spatially directed functionalities make them intriguing building blocks for self-assembled nanostructures. High degrees of functionality and modifiability allow for their assembly via non-covalent interactions, such as electrostatic and coordination bonding, enabling controlled self-assembly into higher-order structures. These assembly processes are sensitive to the molecules used and the surrounding conditions, making it possible to tune the chemical and physical properties of the resultant material and generate multifunctional and environmentally sensitive systems. These materials have numerous potential applications, including catalysis and drug delivery.

Graphical Abstract

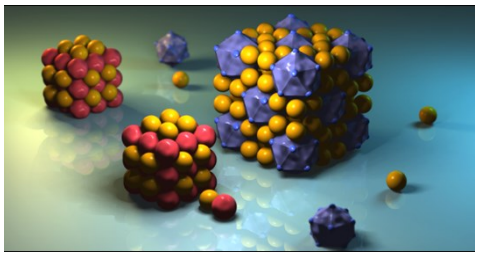

Protein cages, such as viruses (blue) and ferritins (red), can be assembled into higher-order structures with synthetic components (yellow) to produce multifunctional biohybrid materials.

1. INTRODUCTION

The fine structure of materials found in nature greatly exceeds the range of those produced synthetically, both in structural variety, and chemical and mechanical performance. The ability to produce well-defined structures at both the nano and macroscales, and to selectively modify associated functional groups, presents a challenge to modern material science and biomedical technology (DiMarco & Heilshorn, 2012; Wen & Steinmetz, 2016). For decades, scientists have worked to replicate the functional structures found in nature with varying success. In natural systems, material properties originate not only from the chemical composition, but also from the higher-ordered three-dimensional (3D) orientation of linked atomic and molecular compounds, which is dependent on sensitive chemical recognition processes. Following a bottom-up approach, nanostructured moieties are hierarchically incorporated into higher-ordered structures, transferring structures and properties from a nanometer scale to one that can be observed with the naked eye. Unfortunately, majority of these interactions are not sufficiently understood to be able to replicate them in synthetic systems (Sanchez, Arribart, & Giraud Guille, 2005).

Among the building blocks found in nature, proteins are the most functional and versatile biomacromolecules. Protein functions range from structural to catalytic and they are also involved in recognition and transport. Because they are at the center of a vast number of reactions that occur around us, and within our bodies, proteins have been intensively studied for both basic and advanced applications in chemistry and biology. The functionality of an individual protein is largely based on its 3D structure. However, new or enhanced properties can arise from the precise assembly of proteins, such as light-harvesting bacterial and plant photosynthetic antennas. In these suprastructures, chromophore-containing proteins (cytochromes) are spatially arranged with sub-nanometer precision, enabling efficient and multichromatic light absorption. Subsequent transfer of the excitation energy to the reaction center results in charge separation (Qin, Suga, Kuang & Shen, 2015; Yang, Yoon, Yoo, Kim, & Kim, 2012). Some of these protein arrays have reported efficiencies higher than 90% (Nelson, 2009), whereas current solar cell technologies report efficiencies of less than 50% (Green et al., 2018). In fact, over the last two decades a new field of study has emerged that is dedicated to development of new materials based on the positional and orientational control of proteins and conjugation with other functional moieties to create biohybrid materials (Zhang, 2003). The most effective and versatile way to construct these materials is through self-assembly, where separate building blocks are linked together to form highly ordered structures. Natural proteins are ideal for this purpose because their uniform shape and size allows them to assemble into structures with high translational orders, which is essential for producing nanostructured colloidal assemblies (Li et al., 2009), liquid crystals (Flynn, Lee, Peelle, & Belcher, 2003), and crystalline lattices (King et al., 2014). Protein-protein recognition is achieved by a variety of chemical strategies, including covalent bonding, receptor-ligand interaction, host-guest recognition, chemical templating, metal coordination, and electrostatic interaction (Bai, Luo, & Liu, 2016; Luo, Hou, Bai, Wang, & Liu, 2016). Supramolecular approaches present several advantages, such as the employment of native or specifically modified proteins by site-directed mutagenesis with maintained functionality, or the possibility of designing multi-stimuli assembly and disassembly processes, critical in responsive materials.

This review focuses on highly ordered protein suprastructures assembled through supramolecular interactions (i.e., electrostatic interactions, metal-ligand coordination, and self-organization into

liquid crystals). Such materials possess properties that are maintained or enhanced compared to the constituting biomolecules. However, due to the vast amount of protein research in literature, the focus of this review is on highly ordered structures held together by supramolecular interactions. Proteins that have been crystallized for the sole purpose of structural characterization were also excluded to limit the framework to only those proteins with potential applications as functional materials.

This review introduces selected protein cages, with a special focus on geometry due to its key role in determining the overall structure serving as the repeating unit. We divide these protein cages into three main groups: spherical (apoferritin (aFt) and cowpea chlorotic mottle virus (CCMV)), rod-like (tobacco mosaic virus (TMV) and bacteriophage M13), and toroidal (stable protein 1 (SP1), peroxiredoxin (Prxs), and GroEL chaperonin). Next, we describe the different type of assemblies according to the primary driving force (electrostatic, metal coordination, or liquid crystal). Most conjugation agents used are also described in this section, including inorganic nanoparticles (NPs) and divalent cations. Last, we provide an overview of those materials that, in addition to their structure, exhibit promising functionality due to their intrinsic organization.

2. PROTEIN SCAFFOLDS

Several morphologies and functions have been obtained from protein assembly to date. In this review we define a supergroup for 3D protein structures composed of protein subunits as a scaffold, which we limit to spherical, rod-like, and toroidal structures. Because the structures are symmetrical, the variety of subunits per protein scaffold is limited to those fitting the symmetry groups, which promotes the formation of homogeneous assemblies in size and shape. For example, variously shaped, hollow 3D macromolecules composed of peptide chains are called protein cages (Figure 1). These scaffolds consist of a protein shell, also known as the cage, which is constituted by the self-assembly of the corresponding protein subunits. Some hollow cages can encapsulate genetic material from viruses, whereas others, such as ferritin (iron storage) or chaperonins (lipophilic molecules), can encapsulate a broad variety of cargo (Aumiller, Uchida, & Douglas, 2018). Spherical protein cages are rigid, which enhances the regularity of the assembly and introduces porosity into the system, making these cages a research target of interest. Rod-like proteins have also been employed as building block, taking advantage of their anisotropy and high aspect ratio. These scaffolds are typically organized as monodimensional (1D) arrays of coat proteins (CP) encapsulating RNA (Alonso, Górzny, & Bittner, 2013). These rod-like morphologies are known to form liquid crystals at high concentrations, presenting dynamic order. Finally, toroidal protein scaffolds are formed from single or double circular arrays of CPs. In the case of these proteins, no genetic material is packed inside. However, they exhibit enzymatic activity and perform other functions such as assisting in protein folding. Some proteins have a tendency to “pile-up,” resulting in stacks of proteins that can be tuned in length (Phillips et al., 2014; Yewdall et al., 2016). The proteins reviewed in this paper, as well as the types of interactions and co-crystallization agents, are summarized in Table 1.

Table 1: Proteins leading to higher-ordered assemblies, including the driving force and the co-crystallization agent employed.

Protein	Type of interaction	Cocrystallization agent	Reference

aFt	Electrostatic	Au nanoparticles (AuNP)	Kostiainen et al., 2013
		Polypeptides	Bellapadrona et al., 2015; Korpi et al., 2018
		Dendrons and dendrimers	Kostiainen et al., 2011a; Liljeström, Seitsonen, & Kostiainen, 2015; Välimäki et al., 2015
		Protein	Künzle, Eckert, & Beck, 2016; Lach, Künzle, & Beck, 2017
		Small cyclic molecules	Beyeh et al., 2018
		Organic dye	Mikkilä et al., 2016
		Ce^{3+}	Okuda, Suzumoto & Yamashita, 2011
	Coordination bond	$Zn^{2+,}$ $Ni^{2+,}$ Co^{2+}	Bailey, Zhang, Chiong, Ahn, & Tezcan, 2017; Sontz, Bailey, Ahn, & Tezcan, 2015
CCMV	Electrostatic	AuNP	Hassinen, Liljeström, Kostiainen, & Ras, 2015; Kostiainen et al., 2013
		Polypeptides	Korpi et al., 2018; Kostiainen, Hiekkataipale, de la Torre, Nolte, & Cornelissen, 2011b
		Dendrons and dendrimers	Kostiainen, Kasyutich, Cornelissen, & Nolte, 2010; Mikkilä et al., 2013
		Protein	Liljeström, Mikkilä, & Kostiainen, 2014
TMV	Liquid Crystal	Concentration	Bernal & Fankuchen, 1941; Gregory & Holmes, 1965; Lydon, 2014
		Depletion force	Li et al., 2013a; Li, Zan, Winans, Wang, & Lee, 2013b
	Electrostatic	Cationic AuNP	Liljeström et al., 2017
	Coordination bond	Divalent cations	Li, Winans, & Lee, 2011; Nedoluzhko & Douglas, 2001; Schenk et al., 2017
M13 phage	Liquid crystal	Concentration	Adams, Dogic, Keller, & Fraden, 1998; Chung et al., 2011; Dogic & Fraden, 2006; Dogic & Fraden, 1997; Heo et al., 2019; Lee et al., 2017b; Lee, Wood, & Belcher, 2003a; Lee, Lee, & Belcher, 2003b; Yang, Chung, McFarland, & Lee, 2013

		Depletion force: Tween20, Dextran	Gibaud et al., 2012; Lee et al., 2017a
		Phage recognition: quantum dots (QD), streptavidin-labeled AuNPs	Lee et al., 2003a; Lee, Mao, Flynn, & Belcher, 2002
	Electrostatic	Surfactants (DOAB-DDAB)	Liu et al., 2014
		AuNRs	Liu et al., 2015
	Coordination bond	Co^{2+}	Lee, Yun, & Belcher, 2006
SP1	Electrostatic	Quatum dots (QD)	Miao et al., 2014
		Core-crosslinked micelles (CCMs)	Sun et al., 2016
		PAMAM dendrimer	Sun et al., 2015
	Coordination bond	Ni-NTA-AuNPs	Medalsy et al., 2008
TMV discs	Coordination bond	Divalent cations	Bruckman et al., 2011; Zhang, Wang, Zhou, Chen, & Wang, 2018
Prdx	Coordination bond	Ni-NTA-AuNPs	Ardini et al., 2014
GroEL	Coordination bond	Mg^{2+}	Biswas et al., 2013, 2009; Sendai, Biswas, & Aida, 2013; Sim, Miyajima, Niwa, Taguchi, & Aida, 2015; Sim, Niwa, Taguchi, & Aida, 2016

2.1. Spherical protein cages

2.1.1. Apoferritin

Ferritin is a hollow protein cage consisting of 24 subunit proteins, with an outer diameter of 12 nm and an inner cavity of 8 nm. Ferritins can be found in wide variety of life forms, where the function is to balance iron levels by storing and releasing iron at specific sites. An empty ferritin that does not hold iron atoms (or any other atoms or molecules) is referred to as apoferritin (aFt; Figure 1a) and has a total molecular mass of roughly 450 kDa and a negative outer surface in neutral pH (Balla et al., 1992; Häuβler & Farago, 2002). These protein cages differ to some extent in different organisms, e.g. presenting different pore size or assembly/disassembly stimuli, but the overall structure and functionality remain the same. However, these differences can be exploited to produce more environmentally resistant materials. For example, aFt from *Pyrococcus furiosus*, an anaerobic archaeon that resides in volcanic hot springs at temperatures of up to 100°C, can survive in water of this temperature without denaturing, unlike the majority of other cages (Tatur, Hagen, & Matias, 2007). Moreover, aFt can be genetically and chemically modified to possess labels that aim for specific targets. Additionally, the inner cavity can be exploited to carry a wide variety of organic and inorganic cargo (Abe, Maity, & Ueno, 2016).

2.1.2 Cowpea Chlorotic Mottle Virus

Native cowpea chlorotic mottle virus (CCMV) has a roughly spherical protein capsid, with an outer cage diameter of 28 nm and an inner cavity of 18 nm. It is positively charged and encapsulates the RNA genome (Speir et al., 1995; Johnson & Speir, 1997). The CPs self-assemble into an icosahedral capsid with *T = 3* symmetry, consisting of 180 protein subunits with a total molecular mass of approximately 3600 kDa (Figure 1b). The porous capsid allows for the diffusion of small molecules, such as metallic cations, enabling its use as an iron-storage capsid (Douglas et al., 2002). Additionally, CCMV disassembles into the constituting CPs at neutral pH and high ionic strength. After removal of the viral RNA in the presence of $CaCl_2$, the CPs can be reassembled into virus-like particles with the same size and geometry as the native virus (*T = 3*) at pH = 5 (Sikkema et al., 2007), whereas robust smaller capsids (*T = 1*; 18-nm diameter) are obtained in presence of polyanionic species at pH = 7.5 (Lavelle et al., 2009; M. Brasch et al., 2011; Luque et al., 2014). These modular and finely tunable disassembly/reassembly processes render CCMV a powerful biocarrier agent. Additionally, transitions between geometries can be achieved by controlling the aqueous media: the CCMV capsid swells when the pH exceeds 6.5. This rearrangement expands the pores in the capsid and allows small molecules to enter the virus. The process is also reversible; the virus can be shrunk to trap molecules inside, which are later released by controlling the pH. This property makes CCMV ideal for targeted release applications (Douglas & Young, 1998). The virus-like particles of CCMV have been described as nanoreactors, hosting enzymes within the cage (de Ruiter, Putri, & Cornelissen, 2018), and as controlled-release drug-delivery systems (Brasch, Voets, Koay, & Cornelissen, 2013).

2.2. Rod-like proteins

2.2.1. Tobacco Mosaic Virus

Tobacco mosaic virus (TMV) is a rod-like protein cage with outer diameter of 18 nm, an inner channel of 4 nm in diameter, and a length of 300 nm (Figure 1c) (Alonso et al., 2013). TMV is obtained from tobacco plants and was one of the first viruses to be isolated. Native TMV has a total mass of 39.8 MDa and is formed from 2130 identical capsid proteins wrapped around a sequence of single-stranded RNA consisting of 6400 bases. The CPs helically assemble around the viral RNA and this right-handed helix has a pitch of 2.29 nm (Kendall, McDonald, & Stubbs, 2007). At neutral pH, TMV renders a negatively charged surface potential (Alonso et al. 2013). The TMV capsid can also be disassembled into the individual capsid proteins under acidic conditions (Fraenkel-Conrat, 1957). Their reassembly under different buffer conditions yields disks, stacked disks, and helical rods (Klug, 1999). One single dimer disk is formed from two rings of 17 CP each (Butler, 1984). Moreover, TMV capsid proteins have been successfully genetically and chemically modified without disrupting the assembly of the protein cage (Lee et al., 2012; Schlick, Ding, Kovacs, & Francis, 2005).

2.2.2. Phage Virus M13

The wild type bacteriophage M13 is another well-known, rod-like virus, with a length of approximately 900 nm and an outer diameter of 6.5 nm (Figure 1d) (Kehoe & Kay, 2005). Its nucleic acid is a 6470-base, single-stranded DNA sequence that defines the length of the rod-like assembly (van Wezenbeek, Hulsebos, & Schoenmakers, 1980). The 2700 identical major CPs (pVIII) encapsulate the genetic material, and it is capped with five copies of pIX and pVII on one apical position and five copies of pIII and pVI on the other. The proteins can display recognition peptides, which selectively bind to substrates known as phage display (Clackson, Hoogenboom, Griffiths, & Winter, 1991; Kehoe & Kay, 2005; McCafferty, Griffiths, Winter, & Chiswell, 1990; Scott & Smith, 1990; Smith & Petrenko, 1997). The Nobel Prize of Chemistry was awarded in 2018 for this technique, which enables the investigation of protein interactions with peptides/proteins, DNA, and inorganic materials (Smith & Petrenko, 1997; Cao, Yang, & Mao, 2016; Petrenko & Vodyanoy 2003; Schnirman, 2006; Lee et al. 2003a). Additionally, the M13 phage is known to have liquid-crystalline–like behavior in highly concentrated solutions, which will be discussed in further detail in section 3.3 (Dogic & Fraden, 2006).

2.3. Toroidal proteins

2.3.1. Stable Protein 1

Stable protein 1 (SP1) is a plant-based protein commonly isolated from the aspen tree. This toroidal protein results from the assembly of 12 CPs of 108 amino acids into a double-layered, six-membered ring with a total molecular mass of 12.4 kDa (Wang et al., 2003; Wang, Pelah, Alergand, Shoseyov, & Altman, 2002). The SP1 dodecamer assembles via hydrophobic interactions into a 5-nm tall, 11-nm diameter torus with a 3-nm pore (Figure 1e) (Dgany et al., 2004). The SP1 rings have a negatively charged surface at neutral pH, accessible for electrostatic binding (Zhao et al., 2017). SP1 ring-like protein is highly stable at high temperatures (Wang et al., 2006). Furthermore, site-directed mutagenesis of the amino acid sequence allows for selective binding to metal or insulating surfaces (i.e., cysteine to bind to Au and silicon-binding peptide to bind SiO_2, respectively), rendering single-protein monolayers (Heyman et al., 2009).

2.3.2. GroEL

GroEL is part of the chaperonin family and promotes the proper folding of proteins together with its co-chaperonin protein complex, GroEs (Hayer-Hartl, Bracher, & Hartl, 2016). The GroEL of *Escherichia coli* consists of 14 identical subunits (58 kDa each) arranged into two back-to-back, stacked heptameric rings (Braig et al., 1994; Xu, Horwich, & Sigler, 1997). This barrel-shaped capsid has a hydrophobic inner cavity with a diameter of 4.5 nm, an outer diameter of 13.7 nm, and a height of 14.6 nm (Figure 1f) (Braig et al., 1994). Chemical modification of the CP apical position endows a binding motif that allows anisotropic head-to-tail assembly into nanotubes, as further described in section 3.2 (Sim et al., 2016).

2.3.3. Peroxiredoxin

Peroxiredoxins (Prxs) belong to an abundant family of peroxide-dependent antioxidant enzymes within cells (Perkins, Nelson, Parsonage, Poole, & Karplus, 2015; Rhee, Chae, & Kim, 2005). Although Prxs can be found as CP dimers in solution, decameric toroidal capsids with an approximate outer diameter of ∼13 nm, an inner pore of ∼6 nm, and a height of ∼4 nm are more commonly found (Jang et al., 2004; Domigan et al., 2017; Ardini et al., 2014) (Figure 1g). Furthermore, larger aggregates and higher-order complexes such as toroid stacks or spherical cages are naturally found under reducing conditions (Lowther & Haynes, 2011; Phillips et al., 2014). Prxs can be divided into three subgroups based on the number and position of cysteine residues (Perkins et al., 2015), or into a more recent and substantial division of six subfamilies based on their function and structure (Rhee et al., 2005). All types have a conserved cysteine residue in the N-terminal region where the oxidation of H_2O_2 occurs. These proteins act as peroxide regulators and chaperones in mammalian cells, with additional function in the control of cell signaling (Jang et al., 2004). Moreover, Prxs can be reduced back to the original decamer or dimer in presence of sulfiredoxins (Biteau, Labarre, & Toledano, 2003). The natural trend of Prdxs to aggregate into columnar stacks has been exploited by Gerrard's group (Domigan et al., 2017; Phillips et al., 2014; Yewdall et al., 2016), allowing the formation of rod-like iron oxyhydroxide via mineralization of the inner pore with iron citrate, followed by assembly in a mildly acidic pH. This biomimetic approach enables the synthesis of iron-containing particles restricted in size by the protein template (Manuguri et al., 2018).

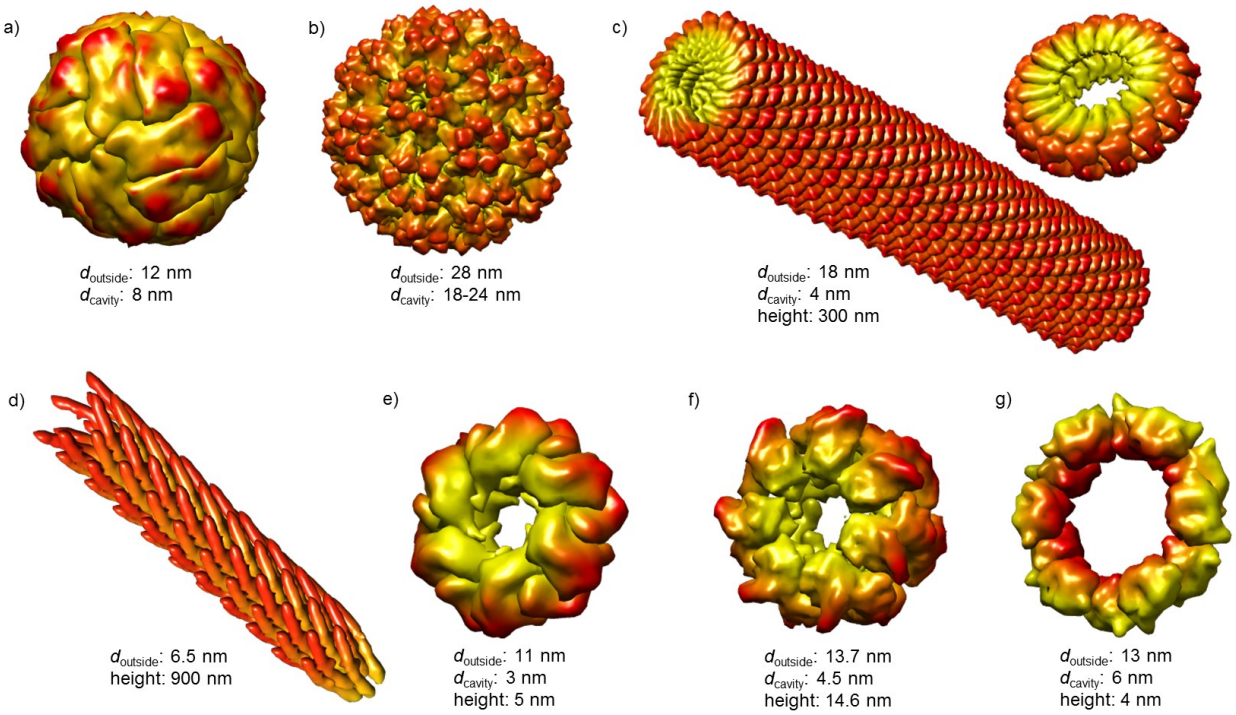

Figure 1. Structural representation and dimensions of a) horse spleen aFt (1IER); b) CCMV (1CWP); c) TMV rod (3J06) and its two-ring circular permutant (3KML); d) M13 phage (1IFI); e) SP1 (1TR0); f) GroEL (1SS8); and g) bovine mitochondrial Prx (1ZYE). Structures (not presented in scale) have been rendered with UCSF Chimera software V1.10.1, employing the structures deposited in the RCSB Protein Data Bank. The red color is indicative of local negative charge, but the coloring is not quantitative.

3. SELF-ASSEMBLY AND HIGHLY ORDERED PROTEIN MATERIALS

The production of nanoscale structures has traditionally been carried out by top-down methods, where larger structures are first prepared and then cleaved into the desired motifs. As effective as the method is, it is limited in terms of structure uniformity and process upscaling (Zhang, 2003). Bottom-up methods, where relatively small particles are arranged into larger systems, are more versatile and have therefore attracted much attention. Self-assembly, where the arrangement occurs spontaneously, is one such process (Toksoz, Acar, & Guler, 2010). Regardless of the size of the self-assembling particles, sufficiently low dispersity and molecular mobility are required to achieve hierarchical structures, as inconsistent particles and a too-fast assembly yield random aggregates (Whitesides & Boncheva, 2002). Self-assembly is most commonly realized in solutions using non-covalent interactions because they are easy to introduce and, in many cases, reversible. The specific orientation adopted by the building blocks depends on their physical and chemical properties, as well as the surrounding media. A major challenge in both nano and macroscale self-assembly is controlling the hierarchical orientation of the assemblies. Additionally, since non-covalent interactions are weaker than covalent ones, more functional sites are required. The interactions include van der Waals, hydrogen bonding, coordination binding, and hydrophobic and ionic interactions—the last being the strongest of these forces, but more difficult to control due to the lack of directionality (Faul & Antonietti, 2003). Hierarchical structures provide enhanced material properties and the possibility of integrating the materials with additional functionalities for applications in electronics, catalysis, and tissue engineering. For this reason, it is meaningful to study

these structures and to try to overcome the difficulties in preparation (Majetich, Wen, & Booth, 2011).

Proteins are one of the most versatile groups of functional building blocks for self-assembling systems at our disposal due to their availability, and programmability by site-directed mutagenesis. Protein-only materials like silk and elastin have been widely studied due to their outstanding chemical and mechanical properties. However, the material pool can be greatly broadened by complexation of proteins and with synthetic molecules. The properties of the material can be tuned according to the desired application by careful selection of the constituting materials. Consequently, the number of compatible building blocks and resulting systems produced is practically unlimited (Huber, Schreiber, Wild, Benz, & Schiller, 2014). High control in the self-assembly process leads to materials that maintain long-distance orientation and position of the building blocks; that is, crystalline structures. The crystalline phase provides rigidity and a confined space, allowing for the possibility of oriented reactions within and between building blocks (Abe et al., 2016). Protein crystals have unique properties compared to uncomplexed starting materials, which have made them the material of choice for numerous researchers across the world. These features include having a porous nature with a uniform cavity size, accessible amino acid residues on surfaces, and promoting synergic effects that improve reactivity (Ding, Shi, & Wei, 2014). The greatest advantage of protein crystals compared to crystals composed of other soft materials is their stereochemistry-based selectivity. Multiple chiral centers are the core of protein functionality that allow the proteins to interact only with specific counter particles. These particles must match the “mold” of the protein at numerous sites, commonly referred to as a lock-and-key interaction. When assembled into a crystal lattice, the locks can force the keys to a specific distance and orientation relative to each other, enabling the production of nanostructures (Borg et al., 2007). The protein functionalities retain high activity due to high accessibility, resulting from the porosity of the structures, even in the center of the crystals. If the crystals are fortified by crosslinking, they also possess high physical rigidity (Vilenchik, Griffith, St. Clair, Navia, & Margolin, 1998).

On the other hand, rod-shaped molecules are known to exhibit liquid-crystalline ordered phases in suspension. This state of the matter provides a certain degree of orientational order, while offering translational freedom. Liquid crystals are subdivided into thermotropic and lyotropic phases, and exhibit temperature-dependent changes in organization, or changes via combination of temperature and concentration (Chandrasekhar, 1992; Collings, 1990). The main thermotropic phases occur in the following increasing range of order: nematic, smectic, and chiral or cholesteric. Whereas the nematic phase provides orientational order by the alignment of the rod-like particles, the smectic and choloesteric phases provide partial translational order of the molecules in layers, presenting the latter a step-wise rotation between layers (Dogic & Fraden, 2006).

Crystalline and other protein-based structures are also associated with certain challenges. They are highly complex in organization and quantitative modification is problematic. The fact that the functionality of a protein is based on its 3D orientation makes having control over modifications even more important, because incorrect or inconclusive modifications could destroy the chemical properties of the protein, which would undermine its purpose. Additionally, proteins are expensive compared to most available synthetic molecules (Szentivanyi, Assmann, Schuster, & Glasmacher, 2009).

3.1. Electrostatic self-assembly

Electrostatic self-assembly is a sound choice for the preparation of higher-order protein structures, because some of the native building blocks, like TMV (Alonso et al., 2013) and CCMV (Prinsen, van der Schoot, Gelbart, & Knobler, 2010) carry negative surface charges near neutral pH. It is also more versatile than might be expected, because the structures obtained depend on the sum of multiple factors, such as the charge density of the assembling particles, size of the co-crystallization agent, shape and dimensions of the protein, and electrolyte concentration of the medium. Self-assembly of protein scaffolds has even been reported in living cells, including insectoid (Koopmann et al., 2012; Abe et al., 2017), mammalian (Bellapadrona & Elbaum, 2014), and bacterial cells (Bellapadrona et al., 2015). Specifically, if the charged building blocks are large molecules, like proteins, they contain multiple charged sites that are rarely distributed evenly on the surface. Such uneven charge patterns can give rise to oriented assembly, which may provide the systems with additional pores (Bishop, Wilmer, Soh, & Grzybowski, 2009). Additionally, electrostatic self-assembly offers the possibility of disassembling the crystal structures by changing the electrolyte concentration or pH, provided that the building blocks have isoelectric points within the range of the pH change. This could be used as a site-specific activation method if some of the building blocks have functionalities that cannot be activated within the crystal, but can be activated once they are free in the medium (Kostiainen et al., 2010).

One drawback of electrostatic self-assembly is that the strength of the interactions must be precisely controlled in order to achieve an ordered structure. Weak interactions fail to assemble the building blocks, and those that are too strong cause rapid and static bonding that lacks spatial regularity. The strength of the interactions is usually tuned by adjusting the concentration of additional electrolytes in the solution, typically a small ionic salt like NaCl. The effect of electrolyte concentration has been demonstrated in the assembly of CCMV in the presence of cationic gold nanoparticles (AuNP) at varying particle ratios and different pH levels (Kostiainen et al., 2013). Crystalline structures were obtained over a wide range of both particle ratios (m_{AuNp}/m_{CCMV} 0.5-2.0) and pHs (3.5-6.0) when a sufficient salt concentration was used to adjust the Debye screening length (κ^{-1}). pH had a particularly significant effect on the κ^{-1} capable of producing crystal lattices, ranging from κ^{-1} 2 nm at pH 3.6 to κ^{-1} 0.8 nm at pH 6.0. Amorphous structures were observed with higher κ^{-1} values and all structures could be reduced to individual particles at a sufficiently high salt concentration. The formation of crystal lattices between AuNPs of various sizes and CCMV has also been shown (Hassinen et al., 2015), as well as between AuNPs and aFt (Kostiainen et al., 2013) and TMV. These capsids typically produces 2D hexagonally packed crystals with AuNPs or dendrimers (Gebhardt et al., 2014; Li et al., 2013a; Riekel, Burghammer, Snigirev, & Rosenthal, 2018; Wu, Jiang, Zan, Lin, & Wang, 2017), but a stepwise decrease in the ionic strength force of the solvent has been reported to induce the assembly of 2D square lattice structures due to the bridging of the particles into four TMV capsids (Liljeström et al., 2017). In this case, the inherent helicity of the capsid was also transferred into the superlattice, leading to the helical arrangement of AuNPs, as characterized by transmission electron cryomicroscopy (cryo-TEM), scanning electron microscopy (SEM), and circular dichroism (CD) features of the plasmonic resonance peak (i.e., the resonant oscillation of the conducting electrons of the NP, which strongly depend on the size) at ~530 nm (Figure 2a). Furthermore, decoration of the fiber-like crystals with Fe_2O_3 NPs rendered magnetoresponsive fibers that aligned under an external magnetic field.

Purely organic electrostatic assemblies of protein scaffolds have been obtained using materials other than AuNPs for complexation, such as polymers (Kostiainen et al., 2011b; Mikkilä et al., 2013). Regardless the selected intermediary particles, the structure of the assemblies remains dependent on the surrounding conditions. The formation of CCMV crystalline structures by complexation with cationic peptide chains fused to green fluorescent protein (GFP) has been shown (Korpi et al., 2018) . The complexes formed face-centered cubic (*fcc)* lattices with GFP in the cavities between the CCMV. The same polypeptides failed to form crystals with aFt because the cavities of the potential crystals were too small to house the GFP (Figure 2b). Both CCMV and aFt formed *fcc* crystals with polypeptides that had not been fused to GFP. Many other systems have also been reported, where intermediary particles of electrostatic protein scaffold assemblies have incorporated additional functional particles besides the cationic groups required for self-assembly. Other proteins are an obvious choice because they have selective functionalities and are chemically similar to protein cages. Avidin has been shown to electrostatically self-assemble into crystals with CCMV in mildly saline aqueous solution (Liljeström et al., 2014). Moreover, the crystals could be further functionalized by molecules tagged and labelled with biotin, which binds effectively and selectively with avidin. This functionalization was demonstrated by incorporating the crystals with fluorescein, horseradish peroxidase enzyme, and AuNPs via biotin-tagging.

Synthetic molecules that are smaller than polymers can also be used to introduce additional functionalities into protein cage assemblies. Cyclophanes are small cyclic molecules capable of trapping even smaller molecules within them by host-guest interactions. By modifying them with a various number of cationic groups attached to the outer edges of the molecules, the cyclophanes have been shown to assemble with aFt in mild electrolyte concentrations (Beyeh et al., 2018). The cyclophanes used were cup-like resorcin[4]arene and tube-like pillar[5]arene with protonated amine groups as cationic sites. Cyclophanes with more than five protonated amines complexed efficiently with aFt. Especially interesting was pillar[5]arene with ten protonated amines, five on each side of the ring, leading to *fcc* lattices (Figure 2c). The cyclophanes fit into the spaces between the aFt cages and the lattice constant was 20.5 nm. The structures were suggested to be multifunctional biohybrid materials, because both cyclophanes and aFT may trap smaller molecules within them and the porous system structure would allow such small particles to diffuse throughout the system. Similar aFt assemblies have been achieved using small supramolecular complexes to obtain the first photoactive materials of this kind (Mikkilä et al., 2016). A cationic photosensitizer (phthalocyanine) and a negatively charged molecule (pyrene) were used to form a supramolecular complex that induced crystallization of aFt in a *fcc* crystal structure with a lattice constant of 19.6 nm, which corresponds to an interprotein distance of 13.6 nm (Figure 2d). The resulting crystals were robust, photoactive biohybrid materials that emitted fluorescence and generated highly reactive $^1O_2$without self-degradation upon irradiation.

Protein scaffold–based materials can also be physically active in addition to having chemical properties. Many hollow scaffolds can be filled with magnetic particles to introduce magnetic responses in addition to the protein properties initially present. Fe_3O_4-γ-Fe_2O_3 iron oxide-encapsulated ferritin (magnetoferritin) has been complexed with dendrons carrying photolabile cationic spermine end groups (Kostiainen et al., 2011a). The particles formed *fcc* lattices with a lattice constant of 13.1 nm and had magnetic properties that differed from those of individual magnetoferritins, because the crystals presented ferromagnet-like properties in opposition to the free particles that were superparamagnetic. The crystals could be disassembled into individual NPs

using ultraviolet (UV) irradiation due to the photolability of the cationic surfaces of the dendrons, making the complexes potential carrier systems (Figure 2e). Similar optically active systems (without magnetic properties) based on CCMV were also demonstrated earlier by some of the same researchers (Kostiainen et al., 2010).

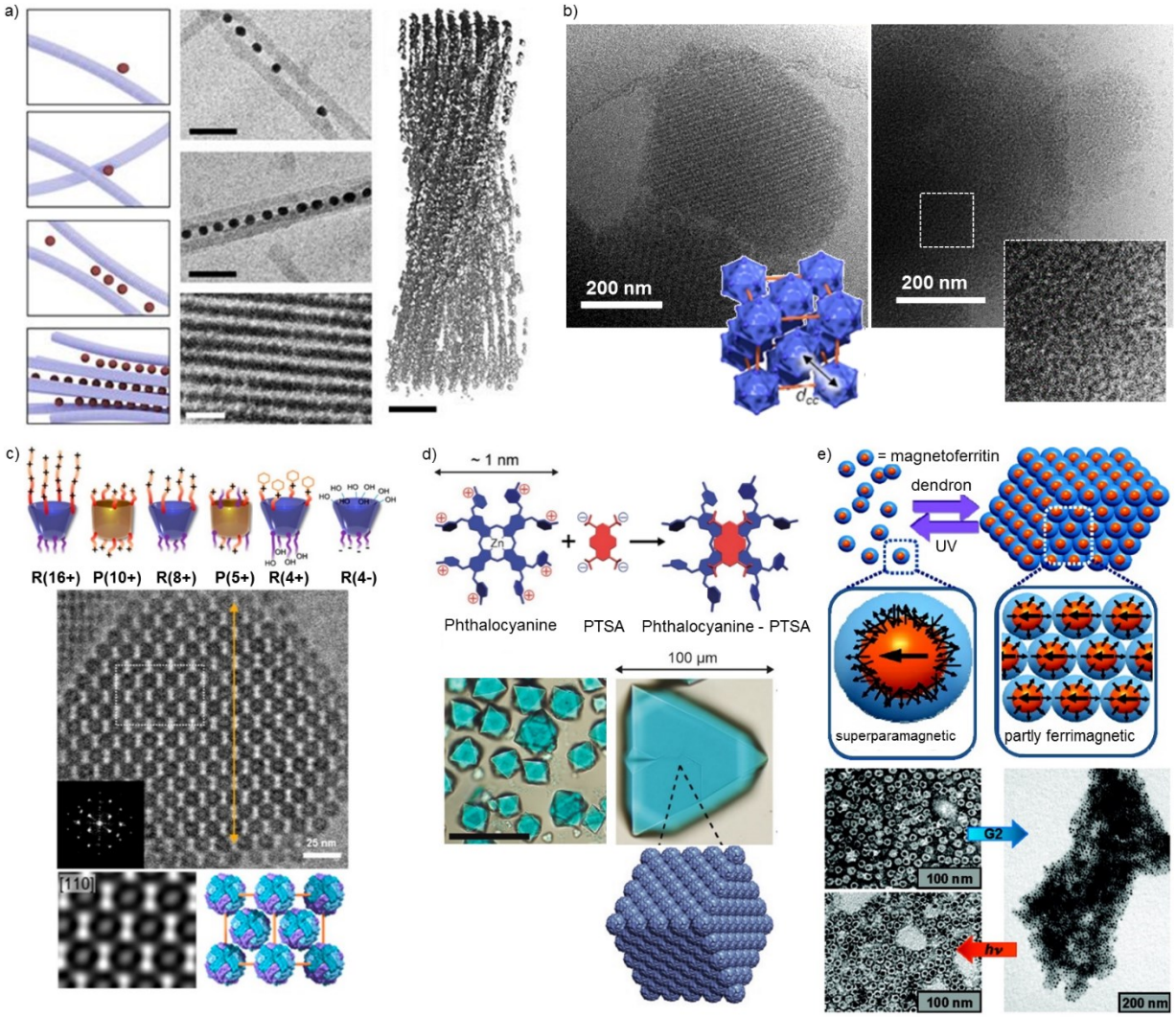

Figure 2. a) TMV and AuNPs. Schematic (left) and cryo-TEM images (middle) of the assemblies with an increasing number of AuNPs (scale bar = 50 nm) and a cryo electron tomographic (cryo-ET) reconstruction of a superlattice wire with a right-handed twist along the wire axis (right; scale bar = 200 nm). b) GFP-K72 with CCMV and aFt. A cryo-TEM image of CCMV-GFP-K72 crystals with a schematic of CCMV packing (left) and amorphous aFt-GFP-K72 complexes (right), with a magnified image of the unoriented structure (right inset). c) Cationic cyclophanes and aFt. Schematic of the studied hosts with the number of charges (top), the cryo-TEM image of the aFT – P(10+) crystal viewed along the [110] projection axis (middle) with a fast Fourier transformation (FTT) of the crystal (middle inset) and an inverse and filtered FTT along the same projection axis (bottom left). A schematic of the crystal structure (bottom right). d) Organic dyes and aFt. Schematic of the organic dyes (top) and optical microscopy images of aFt – phthalocyanine-PTSA crystals at 20 mM NaCl (middle left; scale bar = 50 µm) and 30 mM NaCl solution (middle right) with a schematic of the aFt assemblies. (bottom). e) Optical disassembly of magnetoferritin complexes. Schematic (top) and TEM images (bottom) of free magnetoferritin self-assembly with cationic dendrons and disassembly back to NPs after exposure to UV radiation. Figure adapted with permission from Liljeström et al., (2017), Korpi et al., (2018), Beyeh et al., (2018), Mikkilä et al., (2016), and Kostiainen et al., (2011a).

While rod-like proteins have been typically used to yield anisotropic assemblies, they are not the only geometry suitable for that purpose. Toroidal proteins have been widely used in conjugation with spherical particles to form monodimensional stacks. Quantum dots (QD) are heavily studied particles that are also capable of electrostatic assembly with protein scaffolds, namely negatively charged SP1 protein nanorings and oppositely charged CdTe QDs (Miao et al., 2014). Quantum dots of three different sizes (3-4, 5-6, and 10 nm) coated with cationic ligands induced the self-assembly of SP1 into various nanowires, subsequent bundles, and irregular networks in aqueous solution. Smaller QDs (3.3 and 5.8 nm) induced straight nanowires whereas branching occurred for the larger ones (11.5 nm) due to multiple nanorings connected to the same particle (Figure 3a). Quantum dots exhibit enhanced luminescence in solution due to the spacing between the QDs within the stack. The efficiency of energy transfer between QDs of the same size was above 90%. Furthermore, mixed assemblies between different size QDs (3.3 and 11.5 nm, 50:1 ratio) led to an obvious fluorescence resonance energy transfer (FRET) effect, indicating that the energy was initially transferred among the multiple smaller QDs and then collected by the reaction center of the larger one, constructing a highly efficient light-harvesting system. On the other hand, SP1 has also been arranged into an artificial photosynthetic antenna with core-crosslinked micelles (CCMs) generating 1D assemblies (Sun et al., 2016). The CCMs were synthesized by spontaneous micelle formation of the corresponding cationic surfactant followed by radical polymerization. This resulted in positively charged, 10-nm micelles with high stability against dilution below the critical concentration. Combination of the building blocks in a 1:1 ratio resulted in up to 200-nm long linear stacks with a uniform height of 10.3 nm (Figure 3b). Further labeling of SP1 with an electron donor and CCMs with an electron acceptor chromophore resulted in a good model of bacterial light-harvesting systems. The fluorescence spectra and lifetime measurements showed that the absorbing energy was transferred within adjacent donors around the SP1 ring and collected in a nearby acceptor located in the CCM of the nanowires.

The same research group exploited this strategy again to create multi-enzyme cooperative antioxidative systems (Sun et al., 2015). The assembly of a selenocysteine-modified SP1 ring and porphyrin-containing generation 5 poly(amidoamine) (PAMAM) dendrimers resulted in nanowires in aqueous solution. Mixture at a 1:1 ratio in a low concentration of NaCl (100 mM) rendered fibers over 100-nm long, with uniform height, as characterized by atomic force microscopy (AFM) and TEM (Figure 3c). Importantly, with site-directed mutagenesis of the SP1 ring, the addition of glutathione peroxidase (GPx), and the addition reaction of superoxide dismutase (SOD) on the PAMAM dendrimer surface, the hybrid was designed to exhibit enzymatic responses of both GPx and SOD. This specific modification aimed to replicate the synergistic effect of these enzymes in living systems without hindering the self-assembly process. Indeed, the multi-enzyme mimics showed biological effects that were notable compared to those of single enzymes in protecting mitochondria against oxidative stress, and had low cytotoxicity and good biocompatibility with human cells.

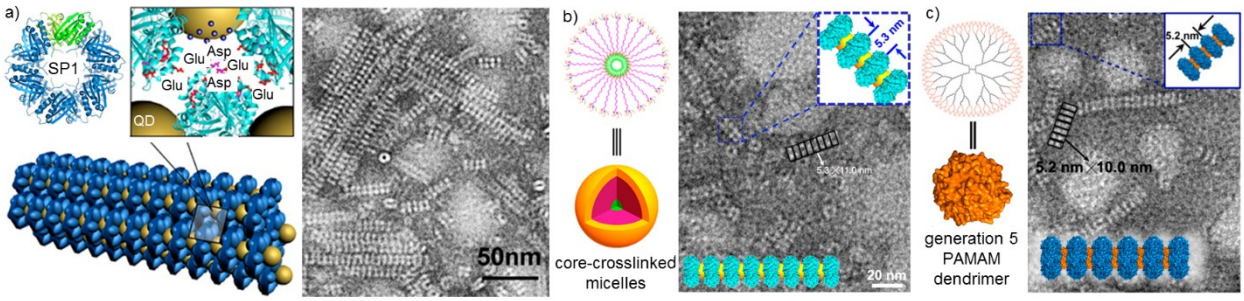

Figure 3. a) Self-assembly of SP1 into monodimensional stacks. Nanowire formed by the self-assembly of SP1 (blue) and QDs (yellow spheres). b) Nanowire composed of SP1 rings (cyan) and CCMs (yellow). c) Assembly model of SP1 and a porphyrin-containing PAMAM dendrimer. Adapted with permission from Miao et al. (2014) and Sun et al. (2015, 2016).

3.2. Coordination bonding via metal-ligand interactions

Even though electrostatic interactions are an effective method for non-covalent self-assembly, they are not the only method of note in natural systems. Transition metals in mid and late groups of the fourth period are commonly present at natural peptide and protein interfaces, where they have dual functionality. First, they act as links between organic particles (also known as a bridging effect) and second, they change the properties of the systems via redox chemistry reactions. Although the role of these metals in proteins has been extensively studied, only more recent improvements in our understanding of these principles have enabled a growing body of research on biohybrid materials. These systems have substantial potential for producing multifunctional and environmentally sensitive materials, but they are complex systems that are difficult to construct in a controllable manner (Sontz, Song, & Tezcan, 2014).

Supramolecular polymers comprised of non-rigid monomers linked together by coordination bonds have a general tendency to form crosslinked systems due to the random motion of the chains. Loose crosslinking dramatically affects the mechanical properties of the material, and is generally not desired because it fails to maximize mechanical strength or porosity. However, protein scaffolds are rigid structures and coordination bonding can be selectively controlled to distinct sites on their shell, which prevents the formation of random coils and crosslinks. Additionally, protein scaffolds provide the system with additional functionalities, allowing for the production of multifunctional biohybrid materials. A drawback of the procedure is that protein modification to incorporate metal chelating groups is needed most of the time (Broomell et al., 2010). Multiple binding sites to a metal ion per protein further increase complex rigidity, favoring crystalline structures. This property is dependent on the ratio of metal ions to proteins, or more accurately to the chelating groups, as a larger relative amount of metal ions gives proteins greater freedom of movement about each bond (Salgado, Lewis, Mossin, Rheingold, & Tezcan, 2009). Additionally, the metal ions Ni^{2+}, Cu^{2+}, and Zn^{2+} have the specific advantage of undergoing reversible ligand substitution, thereby enabling the structure to achieve the thermodynamically most-favorable orientation. Thus, these ions are more likely to produce materials that are chemically and physically stable (Sontz et al., 2014).

aFt has been shown to assemble into various crystal structures depending on the modification of the cages and linker unit between them (Sontz et al., 2015). The amino acid position 122, which lines C3 symmetric pores, was modified to display metal chelating units able to form coordination bonds with tetrahedral ions. The modified ferritins self-assembled with Zn^{2+} ions into face-centered cubic

lattices, but the procedure was also carried out using an organic linker to direct the formation of coordination bonds which resulted in body-centered cubic lattices. The linker used was a rigid linear benzene-1,4-dicarboxylic acid that prevented the ferritins from assembling into the more compact *fcc* structure (Figure 4a). The linker-directed structure was highly porous, with a solvent content of 67%, which makes it a promising candidate for templating inorganic structures. The authors have since experimented with the alternative metal ions Ni^{2+} and Co^{2+}, as well as five dihydroxamate linkers, all resulting in robust crystalline assemblies (Bailey et al., 2017). Similarly, native TMV has been found to crystallize into ordered arrays in the presence of divalent cations (Nedoluzhko & Douglas, 2001; Schenk et al., 2017). Among all of the cations tested, only Ba^{2+} rendered needle-like crystals, tens of microns long. The other cations (Cd^{2+}, Zn^{2+}, Ca^{2+}, Mg^{2+}) formed liquid-like assemblies (Li et al., 2011). Small-angle X-ray scattering (SAXS) analysis of this hybrid showed close hexagonal packing perpendicular to the bundle propagation axis and an inter-virus distance of 21.6 nm. With a TMV diameter of 18 nm, the bridging effect was discarded, whereas a like-charge attraction was found to be the driving force.

Taking advantage of the modularity of TMV CPs to form disk-like assemblies, genetic modification with oligohistidine residues (His-TMV-CP) has led to enhanced stability and new assembly modes. Histidine mutagenesis at the protein termini is a widespread strategy for enabling facile purification while maintaining protein structure and functionality. Oligohistidine residues have a high affinity for divalent cations such as Zn^{2+} or Ni^{2+}, which are immobilized into the solid phase through nitrilotriacetic acid (NTA) derivatives. This bond presents high directionality and has been used to generate 2D arrays in the presence of divalent cations, such as Zn^{2+} and Cu^{2+}, when the solvent-oriented C-terminus position of the TMV CP is modified with a tetrahistidine residue (Figure 4b) (Zhang et al., 2018). Strong coordination between the imidazole groups and the bivalent cations facilitated assembly along the *x*-*y* plane into hexagonal lattices, according to SAXS and electron microscopy results (Figure 4c). The same C-terminus position was similarly modified with a hexahistidine residue that allowed for fine control of morphology by tuning the buffer mixture, temperature, and the Ni-NTA chelating agent (Bruckman et al., 2011). Permutant His-TMV-CP forms toroids in 400 mM phosphate buffer at pH = 7, and further assembly in bidimensional arrays (pH = 6), and exceptionally long and stable monodimensional stacks (pH = 5). These aggregation patterns are a consequence of the histidine-metal bridging effect, with divalent cations present in the buffer. By decreasing the buffer concentration to 100 mM at pH = 5.5, shorter rods are formed that can evolve into elongated rafts over time. Adding a competitive Ni-NTA complex proves the role of the cation in these structures, chelating the oligohistidine residues and subsequently hampering the interprotein interaction. This leads to disassembly of the rafts, eventually yielding rods, discs, and even individual His-TMV-CP.

The histidine-Ni-NTA interaction has also been exploited to assemble stacks of SP1 linked through AuNPs (Medalsy et al., 2008). To this end, the N-terminus region was modified with a hexahistidine oligomer that, pointing towards the inner pore of the dodecamer, bound to a 1.8-nm Ni-NTA modified AuNP. Once bound, the NP located in the inner core served as a linker to generate 1D assemblies (Figure 4d). A NP distance of 4 nm along the stack was observed. Further deletion of 5 aa of each N-terminus before His modification allowed a major protrusion of the NP into the protein due to the bigger pore size, resulting in a shorter NP-NP distance of 3.5 nm, which produced a continuous array of AuNPs. Similarly, Prdx I peapod-like stacks were created in the presence of Ni-NTDA-AuNP (Figure 4e). In this case, the assembly process yielded an effective space between the

AuNPs, which enabled employment of the stacks as colloidal nano-separator devices. In fact, the assembly process evolved only upon binding to ultrasmall (1.6 nm) AuNPs, which could be separated from the bigger ones. A narrower size range of NPs was therefore achieved after release in mild acidic conditions (Ardini et al., 2014).

Stimulus-responsive coordination bonding has also been designed, like photoreconfigurable supramolecular nanotubes based on the head-to-tail interaction of GroEL chaperonin (Sim et al., 2016). This barrel-shaped protein was labeled with multiple photochromic spiropyran (SP) units in their apical domain. Upon exposure to UV light, SP isomerizes into merocyanine (MC), which is able to coordinate with Mg^{2+} cations present in the media (Figure 4f-h). Successive exposure of labeled GroEL protein to UV light and 5 mM of $MgCl_2$ in the presence of radical quencher dithiothreitol (DTT) led to micrometer-long tubes with a width of 15 nm. Disassembly of the tubes was achieved via the addition of EDTA (sequestering the bridging Mg^{2+}) or by exposure to visible light, which isomerized the MC into non-coordinating SP. Further experiments with FRET donor- and acceptor-labeled proteins showed that, under reducing conditions, the mixed homopolymers did not undergo spontaneous shuffling. However, upon disassembly and reassembly by subsequent visible/UV light irradiation, a clear FRET effect was observed as a consequence of heteropolymer formation (Sendai et al., 2013). Importantly, the inherent hosting capacity of the chaperonin proteins was exploited to host denatured proteins (Biswas et al., 2009) or magnetic NPs (Sim et al., 2015), triggering their release upon the previously mentioned stimuli or mechanically-induced release (Biswas et al., 2013). Additionally, 2D hexagonal packaging of toroidal proteins has been described for SP1 (Medalsi et al. 2008) and HSP60s chaperonin (McMillan et al. 2002; McMillan et al. 2005), showing their potential for biotemplating the formation of NP arrays.

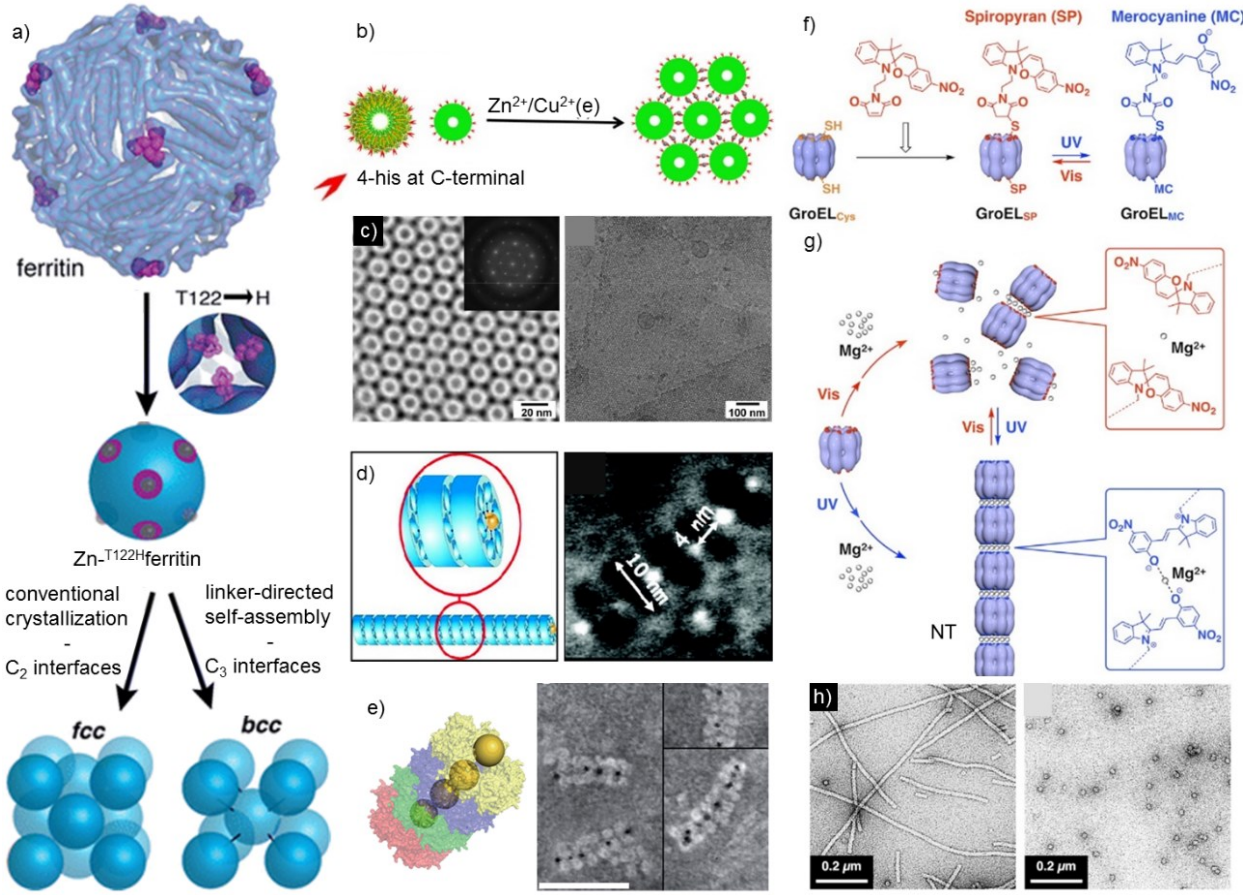

Figure 4. a) Schematic illustration of the assembly of aFt with mutated 122 amino acid sites into *fcc* lattices by conventional crystallization or into *bcc* lattices by interaction between Zn coordination sites and ditopic linkers. b) Schematic illustrations of binding modes of tetrahistidine-modified TMV discs in the presence of metal cations into 2D assemblies. c) TEM and cryo-TEM images of the 2D assemblies. Histidine-modified SP1 (d; left) and Prx (e; left) in the presence of Ni-NTA-AuNPs, and corresponding TEM images showing the peapod structures (d and e; right). f) GroEL carrying multiple spiropyran (SP) units and the reversible photochemical transformation. g) Light-mediated formation and dissociation of the nanotubular assembly (NT). h) TEM images of the assembled (left) and monomeric (right) GroEL proteins. Adapted with permission from Sontz et al. (2015), Zhang et al. (2018), Medalsy et al. (2008) Ardini et al. (2014), and Biswas et al. (2009).

3.3. Self-assembly into liquid crystals

Rod-like particles, including viruses, are well known for forming higher-ordered structures with liquid crystal properties. For instance, native TMV was reported early on to form gels at high concentration (Bernal & Fankuchen, 1941; Gregory & Holmes, 1965; Lydon, 2014). Although the critical concentration needed to form dynamic ordered phases has been lowered by applying forces to the particles, such as shearing flow (Lin, Balizan, Lee, Niu, & Wang, 2010; Wu et al., 2017; Zan, Feng, Balizan, Lin, & Wang, 2013), depletion force (Li, Zan, Sun, et al., 2013; Li et al., 2013b), or as a consequence of drying effects (Gebhardt et al., 2014; Riekel et al., 2018), we do not review them exhaustively here due to space constraints and low developed applicability.

However, materials with liquid crystal properties derived from phages are well known and have been thoroughly studied in the last 20 years. Here, we highlight the findings of some of the most

prominent studies with application potential. Flexible, rod-like M13 phages exhibit liquid crystal properties that strongly depend on phage concentration, ionic strength, and external forces (Adams et al., 1998; Dogic & Fraden, 2006; Dogic & Fraden, 1997; Lee et al., 2003a; Lee et al., 2003b). However, these factors present hierarchically, with concentration playing a major role in solution; (i) M13 phages have been found to behave as individual viruses forming an isotropic (i.e., without any order) phase below 5 mg/mL. Above that concentration, different liquid crystal phases arise with (ii) nematic, between 10-20 mg/mL; (iii) cholesteric, between 20-80 mg/mL; and (iv) smectic phase liquid crystals, above 100 mg/mL (Yang et al., 2013). Control on the chirality of the cholesteric phase formed by these viruses was tuned by controlling the interfacial tension (depletion force) (Gibaud et al., 2012) or the temperature (Liu et al., 2015). The latter employed negatively charged gold nanorods (AuNRs) embedded within the phage-induced chiral phase. The AuNR presented two positive CD peaks at 10°C (705 and 450 nm), the latter being blue-shifted compared to the extinction peak of single AuNRs. This finding was due to the coupling effect between two neighboring AuNRs—the so-called chiro-optical effect. Upon heating, the intensity of the CD signal diminished as a consequence of the decrease of long-range chiral periodic order.

These highly directional structured materials have been extensively studied as 1D scaffolds for a wide variety of organic, inorganic, and biological moieties. The specificity of the M13 phage towards semiconducting materials was described early on (Whaley, English, Hu, Barbara, & Belcher, 2000) and has been used to bind and structure ZnS nanocrystals (Lee et al., 2002); M13 phages displaying ZnS recognition peptides in the pIII minor CP unit bound to nanocrystals in the apical position. Depending on concentration, the M13 phage formed micelles with clustered nanocrystals in their core (0.01%), nematic (22 mg/mL), cholesteric (28-76 mg/mL) with exponential decrease of the pitches by increasing the concentration, and smectic (127 mg/mL) phases. The latter was more ordered, showing constructive and destructive interference patterns of 1 μm, which is in good agreement with the size the bacteriophage (900 nm) aligned in parallel manner, forming a band, and nanocrystal aggregates (20 nm) aligned at the edges of that band. This hypothesis was further confirmed by means of microscopy and diffraction of the different phases. In a similar study, streptavidin-binding viruses were selected to recognize streptavidin-labeled AuNPs, and further scaffolding liquid crystal phases (Lee et al., 2003b). The authors proved the robustness of this approach by modifying the phage itself, attaching two different fluorescent labels, such as fluorescein and phycoerythrin complexes, triggering their self-organization by the addition of streptavidin. These last two publications paved the way for the prolific field of biotemplated materials. Further research involving engineered phages showed bundle formation in the presence of Co^{2+} ions, which were later used to biotemplate Co-Pt alloys with superparamagnetic properties with high anisotropy (Lee et al., 2006). Electrostatic liquid crystals of negatively charged phage and cationic surfactants have also been studied, resulting in a smectic mesophase at 14-58°C. SAXS and wide-angle X-ray scattering (WAXS) analysis laid out a smectic layer reflection (q = 0.0686 $Å^{-1}$) and its harmonics (q = 0.1371, 0.208 $Å^{-1}$) with a periodicity of 91.5 Å (Liu et al., 2014). The latter value was indicative of a bilayer structure, consisting of a sublayer of phage and an interdigitated sublayer of surfactant (c.a. 70 and 21.5 Å, respectively).

4. APPLICATIONS OF PROTEIN ASSEMBLIES

4.1. Scaffolds and linkers

An interesting way of utilizing protein suprastructures is to use them as scaffolds for other materials. This can be achieved via self-assembly of protein scaffolds containing other particles or by soaking particles in solution through a functional protein assembly. In porous protein crystals, the amino acid residues are exposed to the channels within the crystals in a periodical manner and can influence soaking compounds via coordination bonding or chemical modification. However, materials produced this way are limited in that the modifications only occur partially, because the materials otherwise have a tendency to get trapped inside the crystals (Ueno, 2013).

Stimulus-responsive self-assembly of scaffolds can be a powerful tool for producing environmentally sensitive structures that free their building blocks in response to a trigger. Temperature is a convenient switch and has been reported to be applicable for CCMV assembly with a two-block co-polymer (Kostiainen et al., 2011c). The block co-polymer used consisted of cationic poly((2-dimethylamino)ethyl methacrylate) (PDMAEMA) and thermo-responsive poly(diethyleneglycol methyl ether methacrylate) (PDEGMA), and chains with molecular masses of approximately 35 and 17 kDa. The transition temperatures for the two polymers were 36°C and 30.5°C, respectively. The hypothesis was that cationic blocks attach to the surface of CCMV via electrostatic interactions, and below the transition temperature the thermo-responsive block adopts an open conformation and the particles remain soluble. Once the transition temperature is exceeded, PDEGMA collapses onto the surface of CCMV, rendering it hydrophilic, which triggers self-assembly. The systems were studied in an aqueous solution with 30 mg/L of CCMV. At a low electrolyte concentration (i.e., 10 mM of NaCl), neither of the polymers showed a thermoresponsive behavior, where the viruses remained free at 18°C and formed assemblies at 40°C. However, when the electrolyte (NaCl) concentration was increased to 200 mM, both polymers had a concentration window in which the assembly at 40°C occurred. The reversible assembly of nanostructures has potential use in applications in biomedicine; for example, as carrier units. Similar work by the same group of researchers was conducted with aFt combined with a thermo-responsive polymer, yielding hierarchical stimulus-responsive assemblies (Välimäki et al., 2015).

Synthetic dendrimers are a powerful tool for producing biohybrid materials when designed to self-assemble with protein scaffolds. Dendrimers are highly monodisperse particles with high volumes, and their surfaces and pores can often be functionalized, which makes them ideal building blocks. In addition to the chemical nature of the functionalization, the physical location of the site can be set to the outer surface or the inner cavity of the dendrimer, making the system extremely versatile (Setaro et al., 2015). Crystalline assemblies of aFt and PAMAM dendrimers have been reported, where the structure of the assembly depended on the generation of dendrimers used as well as the electrolyte concentration of the solvent (Liljeström et al., 2015). The structures were rigid, due to the fact that they were assembled only from spherical particles. Because the generation of dendrimers has substantial influence on the volume of the particles, it physically limits the dimensions of the arranged structures. The electrolyte concentration of the solution affects the κ^{-1} of the solution, determining the most favorable orientation of the assemblies. Indeed, changing these parameters changed not only the lattice constants, but also the packing model. Dendrimers of generations two and three arranged into *fcc* lattices, and those of generations five to seven arranged into hexagonal packing lattices. However, depending on the electrolyte concentration, generation four dendrimers could adopt both packing models (Figure 5a). The malleability of the structures

makes them useful scaffolds, as the lattice parameters could be fine-tuned depending on the desired properties.

The versatility of protein scaffolds is improved by the fact that even their most fundamental properties can be altered, such as the overall surface charge of aFt (Künzle et al., 2016). Charges were applied by modifying the surfaces of the cages to carry additional amino acid functionalities; specifically lysine and arginine for positive charge and asparagine and glutamine for negative charge. Hence, the natural negative surface charge of ferritin was either enhanced or changed into a positive charge. The slow addition of oppositely charged proteins into a solution at a 1:1 ratio led to the formation of crystalline particles up to 200 µm in diameter. Scaffold properties of the system were demonstrated by encapsulating NPs within either one or both of the protein cages. The positively charged proteins held cerium oxide (CeO_2), and those that were negatively charged held cobalt oxide (CoO). These oxides were chosen due to their applications in catalytic and magnetic materials. A schematic presentation of the systems is shown in Figure 5b. The crystals retained the same structure, regardless of whether one, both or neither of the proteins contained NPs, demonstrating that the particles within the proteins had no influence on the self-assembly. The stability of the crystals was greatly enhanced by crosslinking them using glutaraldehyde. Therefore, the system appears promising for the self-assembly of various inorganic materials in an oriented manner. The same research group studied the efficient encapsulation of cationic AuNPs modified with cargo-loading peptides (CLPs) inside an encapsulin protein cage (Künzle, Mangler, Lach, & Beck, 2018). The protein cage carried binding sites on the inside walls of the cavity, into which the CLPs could bind via lock-and-key interactions. Cargo loading was realized by disassembling and reassembling the encapsulin in different electrolyte concentrations. The cargo loading happened efficiently without CLPs at a lower salt concentration (250 mM NaCl), but not at a higher one (500 mM NaCl), as the electrostatic interactions between the AuNPs and the encapsulin protomers were screened. Using CLP-modified AuNPs, efficient encapsulation was achieved over a wide range of electrolyte concentrations, proving the system to be applicable also in physiological conditions. The CLPs also allowed encapsulation of other than electrically charged cargo.

Proteins of specific shapes that host inorganic particles can be arranged into highly ordered biohybrid materials of distinct lattice structures in order to enhance their physical properties, such as optical activity (Barnes, Dereux, & Ebbesen, 2003) and catalytic efficiency (Daniel & Astruc, 2003). aFt has been used as a synthesis vessel for CeO_2 NP synthesis from $CeCl_3$, demonstrating that even trivalent metal ions can be mineralized in a relatively simple manner by using protein cages (Okuda et al., 2011). Furthermore, the NPs could be arranged into 2D and 3D lattices using Ce^{3+} as linkers between Ce-loaded ferritins, arranging the NPs in a hierarchical manner into potentially catalytically active materials. AuNPs have also been studied for similar arrangement by protein cages. In fact, carboxilated-PEG-modified AuNPs of different diameters have been successfully encapsulated into virus-like particles (VLP) of brome mosaic virus (BMV) (Sun et al., 2007). The highest encapsulation yield (70%) was achieved with an excess of 270 capsid proteins per 12-nm AuNP, resulting in 28-nm, *T = 3* geometry VLPs. Further studies were conducted involving deposition of VLPs into 2D assemblies by the lipid monolayer method, where a diameter reduction (25 nm) was observed compared to the single-particle analysis due to the dense packing of the VLPs. Additional studies were carried out involving 3D crystallization using the hanging drop technique. This approach permitted determination of the lattice constant by atomic force microscopy (AFM; 27.8 nm), much closer to the values obtained by single-particle reconstruction. Additionally, the crystalline structure

showed split absorption bands at 481 and 608 nm, while the monomeric VLPs in solution demonstrated a single absorption peak at 526 nm. This effect was a consequence of the close-packaging in the suprastructure, which led to a multipolar coupling between the Au cores and the subsequent plasmonic band formation. However, protein scaffolds of other geometries are similarly usable. Ring-like proteins have been reported to assemble AuNPs into different hierarchical structures, depending on the size of the NPs (Schreiber, Huber, Cölfen, & Schiller, 2015). The protein acts as an adapter between the NPs, which differs from a typical scaffold system; in this case, the proteins are linked to the NPs but not to each other, because both particles have roughly the same 3D size. Worm-like assemblies have been observed when proteins and NPs were present in equal amounts, and an excess of protein led to branched structures. The assembly occurs due to attraction between the thiol groups of the proteins and NPs, triggering dipole formation. The dipoles are then assembled together to form 1D structures (Figure 5c). The chains that form could be attached to the surface of significantly larger NPs to produce octopus-like structures. With control over the accuracy of such systems, it would be possible to incorporate functional sites in an ordered manner to house cascade reactions or produce biosensors.

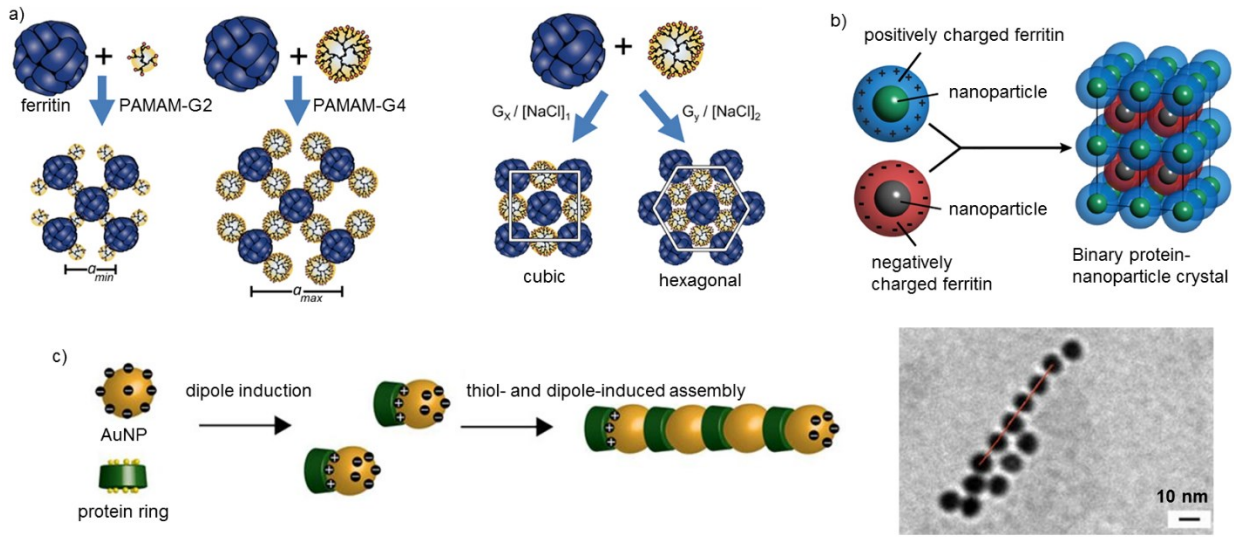

Figure 5. Protein-directed assembly. a) Dendrimer size can be used to control the crystal lattice constant *a*. The dendrimer generation (G) and ionic strength [NaCl] present at the assembly affect crystal symmetry. b) Self-assembly of NP-loaded ferritin cages yield highly ordered 3D superlattices. c) Ring-like proteins bind AuNPs through thiol-anchoring points and induce anisotropic ligand distributions, which result in dipole formation. Multiple dipole-dipole interactions and thiol binding lead to stable AuNP chains (TEM micrograph on right). Adapted with permission of Liljeström et al. (2015), Künzle et al. (2016), and Schreiber, Huber, Cölfen, & Schiller (2015).

4.2. Catalysis

Porous protein crystals are capable of functioning as heterogeneous catalysts with high selectivity and functionality over a wide range of environmental conditions. Specific modification of such structures is challenging, because modification of proteins tends to compromise their ability to assemble in an ordered manner. However, modification is possible, as described in the previous section (Künzle et al., 2016). Indeed, the process has been adapted further as a catalysis system by the same group (Lach et al., 2017). CeO_2 and iron oxide (Fe_2O_3) NPs were synthesized within

negatively and positively charged aFt, which were electrostatically assembled into crystalline lattices. CeO_2-encapsulated aFt was capable of oxidase-like behavior in the absence of hydrogen peroxide (H_2O_2) and peroxidase-like behavior with H_2O_2 present, whereas aFt with Fe_2O_3 could only perform peroxidase-like behavior. Both positive and negative CeO_2-aFt were found to be effective catalysts when free in solution, but positive CeO_2-aFt was found to be more effective due to its greater number of encapsulated metal ions. The crystals, which were several hundred micrometers in size and had been crosslinked to prevent disassembly during the experiments, were more effective because the local concentration of the catalyst was high within the crystals (Figure 6a).

In addition to catalysis, protein scaffolds can perform other simultaneous functions in chemical reactions. Polymerization of phenylacetylene and its derivatives has been reported inside individual aFt cages containing rhodium(norbornadiene) (Rh(nbd)) as a catalyst (Abe et al., 2009). In addition to acting as a catalyst, the cage contributed to the control of polymerization by acting as a physical limiter. Under the study conditions, polymerization was not catalyzed in the absence of Rh(nbd). Without aFt, the reaction was uncontrolled and yielded water-insoluble poly(phenylacetylene), likely due to gelation. However, Rh(nbd)-aFt complexes produced linear water-soluble polymers. aFt could also be used to exclude additional monomers because polymerization of phenylacetylene derivatives carrying carboxylic or phosphonic acid substitutes was not catalyzed by Rh(nbd)-aFt, probably because the anionic monomers could not diffuse into the aFt cages through the negatively charged capsids. Similarly, a size-selective hydrogenation biocatalyst was reported by constructing Pd nanoclusters inside aFt (Ueno et al., 2004). Pd^{2+} diffused into aFt as tetrachloropalladate ions and was reduced to Pd^0, which clustered together and was confined within aFt. Pd^0 outside the proteins was removed by size-exclusion chromatography. The encapsulated clusters were observed to effectively catalyze olefins in aqueous media and remain active after the reaction. The same research group also utilized a modified aFt for Au^{3+} ion accumulation and reduction (Maity, Abe, & Ueno, 2017). These Au immobilized protein scaffolds were first crystallized and crosslinked to maintain the crystal structure during the reduction step. Formation of the nanocluster and stepwise nucleation was followed to fully understand the biomineralization that occurred (Figure 6c).

Protein scaffolds have also been utilized for enzyme encapsulation to attain catalytically active individual icosahedral protein capsids, which can be further assembled into 3D arrays (Uchida et al., 2018). To achieve ordered arrays with face-centered cubic lattices, the outer surface of the capsid was modified to display a negative surface charge, which enabled electrostatic self-assembly with positively charged PAMAM dendrimers. This self-assembly of the protein capsid with two separately encapsulated enzymes provided a functional superlattice material for isobutanol synthesis (Figure 6 b).

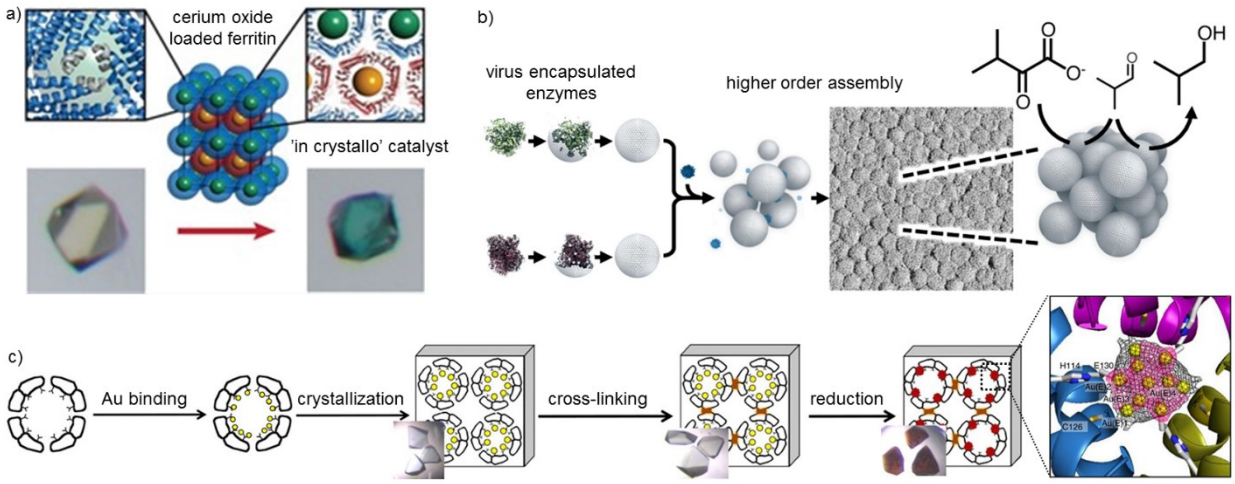

Figure 6. Protein cage crystals for catalysis. a) Metal oxide NPs hosted inside ferritin crystals are accessible for a range of substrates and show oxidase-like and peroxidase-like catalytic activity. b) Enzymes encapsulated inside viruses are catalytically active even when organized into 3D arrays. c) Au atoms can be bound inside a ferritin cage and crystallized together with the cage. Crosslinking treatment of a single crystal enables structural characterization of the formation of a sub-nanocluster via a reduction reaction. Adapted with permission from Lach et al. (2017), Uchida et al. (2018), and Ueno et al. (2004).

4.3. Coatings

Self-assembling systems offer the possibility of depositing specific layer-by-layer coatings of long-range organization on surfaces. Different driving forces can be applied to achieve these coatings, but the interactions are typically non-covalent. Such coatings have potential applications in bioelectronics, for example (Pallarola et al., 2012). Stimulus-responsive coatings are especially interesting because they can often be fine-tuned for practical applications. Light-sensitive coatings based on aFt and synthetic dendrimers have been reported, where the surface patterning could be changed by an external stimulus (Koskela et al., 2014). This functionality arose from azobenzene ethyl orange in the dendrimers. Dendrimers up to generation nine formed surface patterns under illumination by a laser light with a wavelength of 488 nm when spin-coated into films with thickness of a few hundred nanometers. This result was impressive, considering the high (almost 900 kDa) molecular mass of the dendrimers. Patterns of linear streaks and grids were obtained and the patterning was polarization-dependent, which confirmed that the reversible process was triggered by light and not evidence of another phenomenon, like photodegradation. Similar behavior was demonstrated for aFt molecules, which were incorporated with ethyl orange. aFt has a smaller molecular mass than the dendrimers but is closer to a hard sphere in its properties. Streaked patterns in thin electro-spun protein films were obtained under illumination, as shown in Figure 7a.

The natural tendency of the M13 phage to selectively bind to a substrate and then self-template into liquid crystals (Figure 7b) has been successfully exploited to create higher-ordered deposition patterns by pulling a surface from a liquid phase containing different phage concentrations (Chung et al., 2011; Lee et al., 2017b), as shown in Figure 7c. At the triple interphase, the evaporation proceeded faster, causing the local concentration to increase. Control of the phage concentration rendered four different organization patterns: nematic (0.1-0.2 mg/mL), alternate cholesteric/nematic ridges and grooves (0.2-1.5 mg/mL), cholesteric (0.25-0.5 mg/mL), and smectic

helicoidal nanofilaments (4-6 mg/mL). In addition, these structures were further tuned by the pulling speed, ionic concentration, chemistry of the phage surface, and properties of the substrate surface, as shown in Figure 7d (Heo et al., 2019). Control of the ionic strength tunes phage deposition periodicity along the meniscus line, whereas pulling speed controls the continuity of the deposits parallel to the pulling direction. The authors reported fine control of the deposition of 2D arrays of virus at low ionic strengths and high pulling speeds, which exhibits piezoelectric properties. The same technique was used in presence of a surfactant that generated depletion force to deposit hexagonally packed, columnar smectic structures onto gold surfaces (Lee et al., 2017a). These matrices exhibited brilliant colors that depended on the bundle diameter, primarily controlled by the pulling speed (Figure 7e). Increasing the pulling speed decreased the diameter of the fiber, which reflected light at shorter wavelengths (blue). On the other hand, slower pulling speeds increased the fiber diameter, leading to the reflection of longer-wavelength (red) light. These surfaces were employed as colorimetric sensors to detect variation in the relative humidity and to detect benzene, toluene, xylene, and aniline (BTXA) gases by taking advantage of induced selectivity of the phages. The latter use resulted in sensors with applicability in the petrochemical industry.

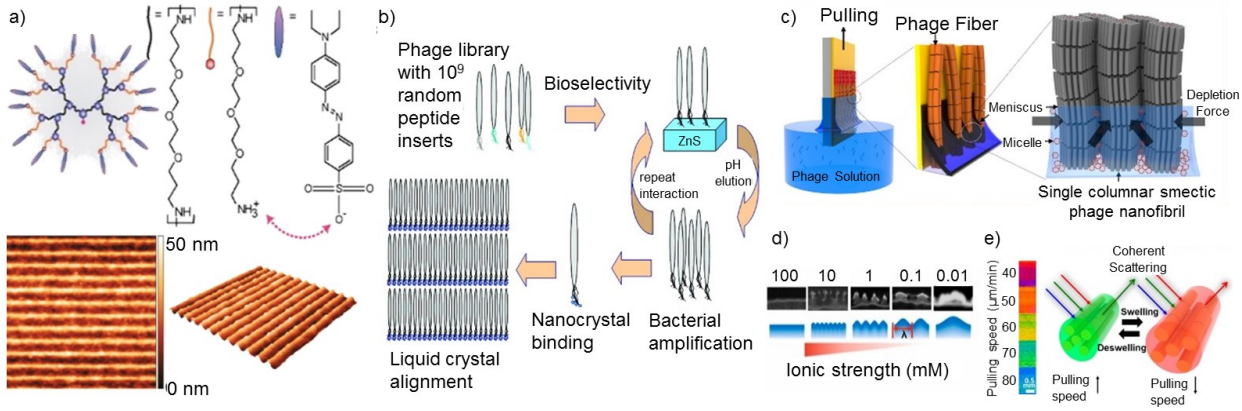

Figure 7. a) Schematic representations of light-sensitive dendrimers (top), an atomic force microscopy height image (bottom left), and a 3D representation (bottom right) of aFt functionalized with ethyl orange. b) Schematic representation of the phage-display strategy for recognizing specific semiconductors, followed by NP synthesis by nucleation and subsequent organization in liquid crystals. c) Surface deposition of phages in controlled patterns by the pulling method. d) Liquid-surface-air profile of the phages, according to the ionic strength of the media. e) Light-absorbing properties of the deposited surfaces, according to thread diameter. Figure adapted with permission from Koskela et al. (2014), Heo et al. (2019), Lee, Fan, et al. (2017), and Lee et al. (2002).

5. Conclusion

Proteins are outstanding building blocks for the creation of new materials that can take advantage of their many features. First, their near monodisperse size and shape allow for robust assembly into periodic structures. Indeed, the high diversity of natural proteins alone means that there is an almost infinite toolkit available to be exploited. Second, the presence of functional groups on the surfaces of proteins enables full control of assembly mode by means of pH, ionic strength, and the presence of cations, as well as external inputs such as magnetic fields or light. Third, the inherent

functionalities of single proteins are not only maintained in the structure, but are usually increased by the incorporation of other materials into the protein scaffold, resulting in highly functional biohybrid materials. Last, materials derived from proteins offer other advantages, such as enhanced biocompatibility and biodegradability. In addition, in most cases these materials can be produced in environmentally sustainable manner.

This review started by addressing the main advantage of using native protein as building blocks for supracolloidal assemblies. Examples of slightly modified proteins are given as well, with the aim of enabling convenient binding positions through site-directed mutagenesis. Current trend in protein modification lays, in fact, in the *de novo* design of proteins (Huang, Boyken, & Baker, 2016). This approach aims to predict by computation new folding structures derived from the protein chain sequence. Even if the *de novo* design of proteins is a challenging approach, the first steps towards such proteins have been already achieved (Joh et al., 2014). We hypothesize that these newly designed proteins have the potential to be incorporated into highly-ordered structures, opening the field to property-enhanced materials.

In this review we focused in the supramolecular assembly of proteins by means of electrostatic, metal-binding, and liquid crystal interactions. These bottom-up approaches transfer individual nanometer-size features across orders of magnitude to the macroscale, while preserving the reversibility of the assembly. We classified the proteins reviewed as corresponding to three main groups according to their geometry (spherical, rod-like, or toroidal proteins). Whereas spherical cages primarily assemble in 3D crystals, the anisotropy of rod-shaped and toroidal proteins form 1D assemblies or stacks. By means of surface deposition and strategic site-directed mutagenesis, 2D arrays have also been reported. Three main application areas of protein-based materials can be identified as follows: protein crystals that act as linkers, catalytic agents, and coatings. These developments highlight the potential for protein-based materials to complement or even replace traditional materials based on their more precise and environmentally benign qualities.

Funding Information

The financial support through the Academy of Finland (267497, 286845, 308578) and Sigrid Jusélius Foundation is gratefully acknowledged. E.A.-P. acknowledges the funding from the European Union's Horizon 2020 research and innovation programme under the Marie Sklodowska-Curie grant agreement No 794536.

Research Resources

This work was carried out under the Academy of Finland Centers of Excellence Programme (2014-2019)

References

Abe, S., Hirata, K., Ueno, T., Morino, K., Shimizu, N., Yamamoto, M., … Watanabe, Y. (2009). Polymerization of Phenylacetylene by Rhodium Complexes within a Discrete Space of apo-Ferritin. *Journal of the American Chemical Society*, *131*(20), 6958–6960. https://doi.org/10.1021/ja901234j

Abe, S., Maity, B., & Ueno, T. (2016). Design of a confined environment using protein cages and crystals for the development of biohybrid materials. *Chemical Communications*, *52*(39), 6496–6512. https://doi.org/10.1039/C6CC01355D

Abe, S., Tabe, H., Ijiri, H., Yamashita, K., Hirata, K., Atsumi, K., … Ueno, T. (2017). Crystal Engineering of self-assembled porous protein materials in living cells. ACS Nano, 11(3), 2410-2419. https://doi.org/10.1021/acsnano.6b06099

Adams, M., Dogic, Z., Keller, S. L., & Fraden, S. (1998). Entropically driven microphase transitions in mixtures of colloidal rods and spheres. *Nature*, *393*(6683), 349–352. https://doi.org/10.1038/30700

Alonso, J. M., Górzny, M. Ł., & Bittner, A. M. (2013). The physics of tobacco mosaic virus and virus-based devices in biotechnology. *Trends in Biotechnology*, *31*(9), 530–538. https://doi.org/10.1016/j.tibtech.2013.05.013

Ardini, M., Giansanti, F., Di Leandro, L., Pitari, G., Cimini, A., Ottaviano, L., … Ippoliti, R. (2014). Metal-induced self-assembly of peroxiredoxin as a tool for sorting ultrasmall gold nanoparticles into one-dimensional clusters. *Nanoscale*, *6*(14), 8052. https://doi.org/10.1039/c4nr01526f

Aumiller, W. M., Uchida, M., & Douglas, T. (2018). Protein cage assembly across multiple length scales. *Chemical Society Reviews*, *47*(10), 3433–3469. https://doi.org/10.1039/C7CS00818J

Bai, Y., Luo, Q., & Liu, J. (2016). Protein self-assembly via supramolecular strategies. *Chemical Society Reviews*, *45*(10), 2756–2767. https://doi.org/10.1039/C6CS00004E

Bailey, J. B., Zhang, L., Chiong, J. A., Sunhyung, A., Tezcan, F. A. (2017). Synthetic Modularity of Protein-Metal-Organic Frameworks. Journal of the American Chemical Society, 139(24), 8160-8166. https://doi.org/10.1021/jacs.7b01202

Balla, G., Jacob, H. S., Balla, J., Rosenberg, M., Nath, K., Apple, F., … Vercellotti, G. M. (1992). Ferritin: A Cytoprotective Antioxidant Strategem of Endothelium. *The Journal of Biological Chemistry*, *267*(25), 18148–18153.

Barnes, W. L., Dereux, A., & Ebbesen, T. W. (2003). Surface plasmon subwavelength optics. *Nature*, *424*(6950), 824–830. https://doi.org/10.1038/nature01937

Bellapadrona, G., & Elbaum, M. (2014). Supramolecular Protein Assemblies in the Nucleus of Human Cells. *Angewandte Chemie International Edition*, *53*(6), 1534–1537. https://doi.org/10.1002/anie.201309163

Bellapadrona, G., Sinkar, S., Sabanay, H., Liljeström, V., Kostiainen, M., & Elbaum, M. (2015). Supramolecular Assembly and Coalescence of Ferritin Cages Driven by Designed Protein–Protein Interactions. *Biomacromolecules*, *16*(7), 2006–2011. https://doi.org/10.1021/acs.biomac.5b00435

Bernal, J. D., & Fankuchen, I. (1941). X-RAY AND CRYSTALLOGRAPHIC STUDIES OF PLANT VIRUS PREPARATIONS : I. INTRODUCTION AND PREPARATION OF SPECIMENS II. MODES OF AGGREGATION OF THE VIRUS PARTICLES. *The Journal of General Physiology*, *25*(1), 111–146.

Beyeh, N. K., Nonappa, Liljeström, V., Mikkilä, J., Korpi, A., Bochicchio, D., … Kostiainen, M. A. (2018). Crystalline Cyclophane–Protein Cage Frameworks. *ACS Nano*, *12*(8), 8029–8036. https://doi.org/10.1021/acsnano.8b02856

Bishop, K. J. M., Wilmer, C. E., Soh, S., & Grzybowski, B. A. (2009). Nanoscale Forces and Their Uses in Self-Assembly. *Small*, *5*(14), 1600–1630. https://doi.org/10.1002/smll.200900358

Biswas, S., Kinbara, K., Niwa, T., Taguchi, H., Ishii, N., Watanabe, S., … Aida, T. (2013). Biomolecular robotics for chemomechanically driven guest delivery fuelled by intracellular ATP. *Nature Chemistry*, *5*(7), 613–620. https://doi.org/10.1038/nchem.1681

Biswas, S., Kinbara, K., Oya, N., Ishii, N., Taguchi, H., & Aida, T. (2009). A Tubular Biocontainer: Metal Ion-Induced 1D Assembly of a Molecularly Engineered Chaperonin. *Journal of the American Chemical Society*, *131*(22), 7556–7557. https://doi.org/10.1021/ja902696q

Biteau, B., Labarre, J., & Toledano, M. B. (2003). ATP-dependent reduction of cysteine–sulphinic acid by *S. cerevisiae* sulphiredoxin. *Nature*, *425*(6961), 980–984. https://doi.org/10.1038/nature02075

Borg, N. A., Wun, K. S., Kjer-Nielsen, L., Wilce, M. C. J., Pellicci, D. G., Koh, R., … Rossjohn, J. (2007). CD1d–lipid-antigen recognition by the semi-invariant NKT T-cell receptor. *Nature*, *448*(7149), 44–49. https://doi.org/10.1038/nature05907

Braig, K., Otwinowski, Z., Hegde, R., Boisvert, D. C., Joachimiak, A., Horwich, A. L., & Sigler, P. B. (1994). The crystal structure of the bacterial chaperonin GroEL at 2.8 Å. *Nature*, *371*(6498), 578. https://doi.org/10.1038/371578a0

Brasch, M., de la Escosura, A., Ma, Y., Uetrecht, C., Heck, A. J. R., Torres, T., & Cornelissen, J. J. L. M. (2011). Encapsulation of phthalocyanine supramolecular stacks into virus-like particles. Journal of the American Chemical Society, 133(18), 6878-6881. https://doi.org/10.1021/ja110752u

Brasch, M., Voets, I. K., Koay, M. S. T., & Cornelissen, J. J. L. M. (2013). Phototriggered cargo release from virus-like assemblies. *Faraday Discussions*, *166*, 47. https://doi.org/10.1039/c3fd00088e

Broomell, C. C., Birkedal, H., Oliveira, C. L. P., Pedersen, J. S., Gertenbach, J.-A., Young, M., & Douglas, T. (2010). Protein cage nanoparticles as secondary building units for the synthesis of 3-dimensional coordination polymers. *Soft Matter*, *6*(14), 3167. https://doi.org/10.1039/c0sm00039f

Bruckman, M. A., Soto, C. M., McDowell, H., Liu, J. L., Ratna, B. R., Korpany, K. V., … Blum, A. S. (2011). Role of Hexahistidine in Directed Nanoassemblies of Tobacco Mosaic Virus Coat Protein. *ACS Nano*, *5*(3), 1606–1616. https://doi.org/10.1021/nn1025719

Butler, P. J. G. (1984). The Current Picture of the Structure and Assembly of Tobacco Mosaic Virus. *Journal of General Virology*, *65*(2), 253–279. https://doi.org/10.1099/0022-1317-65-2-253

Cao, B. Yang, M., & Mao, C. (2016). Phage as a genetically modifiable supramacromolecule in chemistry, materials and medicine. *Accounts of Chemical Research, 49*, 1111-1120. http://dx.doi.org/10.1021/acs.accounts.5b00557

Chandrasekhar, S. (1992). *Liquid crystals* (2nd ed). Cambridge [England] ; New York, NY, USA: Cambridge University Press.

Chung, W.-J., Oh, J.-W., Kwak, K., Lee, B. Y., Meyer, J., Wang, E., … Lee, S.-W. (2011). Biomimetic self-templating supramolecular structures. *Nature*, *478*(7369), 364–368. https://doi.org/10.1038/nature10513

Collings, P. J. (1990). *Liquid crystals: nature's delicate phase of matter*. Princeton, N.J: Princeton University Press.

Clackson, T., Hoogenboom, H. R., Griffiths, A. D., & Winter, G. (1991). Making antibody fragments using phage display libraries. *Nature*, *352*(6336), 624–628. https://doi.org/10.1038/352624a0

Daniel, M.-C., & Astruc, D. (2003). Gold Nanoparticles: Assembly, Supramolecular Chemistry, Quantum-Size-Related Properties, and Applications toward Biology, Catalysis, and Nanotechnology. *Chemical Reviews*, *104*(1), 293–346. https://doi.org/10.1021/cr030698+

Dgany, O., Gonzalez, A., Sofer, O., Wang, W., Zolotnitsky, G., Wolf, A., … Almog, O. (2004). The Structural Basis of the Thermostability of SP1, a Novel Plant (Populus tremula) Boiling Stable Protein. *Journal of Biological Chemistry*, *279*(49), 51516–51523. https://doi.org/10.1074/jbc.M409952200

DiMarco, R. L., & Heilshorn, S. C. (2012). Multifunctional Materials through Modular Protein Engineering. *Advanced Materials*, *24*(29), 3923–3940. https://doi.org/10.1002/adma.201200051

Ding, Y., Shi, L., & Wei, H. (2014). Protein-directed approaches to functional nanomaterials: a case study of lysozyme. *J. Mater. Chem. B*, *2*(47), 8268–8291. https://doi.org/10.1039/C4TB01235F

Dogic, Z. & Fraden, S. (2006). Ordered phases of filamentous viruses. *Current Opinion in Colloid & Interface Science*, *11*(1), 47–55. https://doi.org/10.1016/j.cocis.2005.10.004

Dogic, Z. & Fraden, S. (1997). Smectic Phase in a Colloidal Suspension of Semiflexible Virus Particles. *Physical Review Letters*, *78*(12), 2417–2420. https://doi.org/10.1103/PhysRevLett.78.2417

Domigan, L. J., Ashmead, H., Dimartino, S., Malmstrom, J., Grant Pearce, F., Blunt, M., … Gerrard, J. A. (2017). Formation of supramolecular protein structures on gold surfaces. *Biointerphases*, *12*(4), 04E405. https://doi.org/10.1116/1.4986053

Douglas, T., Strable, E., Willits, D., Aitouchen, A., Libera, M., & Young, M. (2002). Protein Engineering of a Viral Cage for Constrained Nanomaterials Synthesis. *Advanced Materials*, *14*(6), 415–418. https://doi.org/10.1002/1521-4095(20020318)14:6<415::AID-ADMA415>3.0.CO;2-W

Douglas, T., & Young, M. (1998). Host-guest encapsulation of materials by assembled virus protein cages. *Nature*, *393*(6681), 152–155.

Faul, C. F. J., & Antonietti, M. (2003). Ionic Self-Assembly: Facile Synthesis of Supramolecular Materials. *Advanced Materials*, *15*(9), 673–683. https://doi.org/10.1002/adma.200300379

Flynn, C. E., Lee, S.-W., Peelle, B. R., & Belcher, A. M. (2003). Viruses as vehicles for growth, organization and assembly of materials. Acta Materialia, 51(19), 5867-5880. https://doi.org/10.1016/j.actamat.2003.08.031

Fraenkel-Conrad, H. (1957). Degradation of tobacco mosaic virus with acetic acid. Virology, 4(1), 1-4. https://doi.org/10.1016/0042-6822(57)90038-7

Gebhardt, R., Teulon, J.-M., Pellequer, J.-L., Burghammer, M., Colletier, J.-P., & Riekel, C. (2014). Virus particle assembly into crystalline domains enabled by the coffee ring effect. *Soft Matter*, *10*(30), 5458–5462. https://doi.org/10.1039/C4SM00414K

Gibaud, T., Barry, E., Zakhary, M. J., Henglin, M., Ward, A., Yang, Y., … Dogic, Z. (2012). Reconfigurable self-assembly through chiral control of interfacial tension. *Nature*, *481*(7381), 348–351. https://doi.org/10.1038/nature10769

Green, M. A., Hishikawa, Y., Dunlop, E. D., Levi, D. H., Hohl-Ebinger, J., Yoshita, M., & Ho-Baillie, A. W. Y. 2018. Solar cell efficiency tables (Version 53). Progress in Photovoltaics: Research and Applications, 27(1), 3-12. https://doi.org/10.1002/pip.3102

Gregory, J., & Holmes, K. C. (1965). Methods of preparing orientated tobacco mosaic virus sols for X-ray diffraction. *Journal of Molecular Biology*, *13*(3), 796-IN15. https://doi.org/10.1016/S0022-2836(65)80145-0

Hassinen, J., Liljeström, V., Kostiainen, M. A., & Ras, R. H. A. (2015). Rapid Cationization of Gold Nanoparticles by Two-Step Phase Transfer. *Angewandte Chemie International Edition*, *54*(27), 7990–7993. https://doi.org/10.1002/anie.201503655

Häußler, W., & Farago, B. (2002). Diffusive dynamics of ordered solutions of apoferritin near the structure factor peak. *Journal of Physics Condensed Matter*, *15*(1), S197–S204. https://doi.org/10.1088/0953-8984/15/1/325

Hayer-Hartl, M., Bracher, A., & Hartl, F. U. (2016). The GroEL–GroES Chaperonin Machine: A Nano-Cage for Protein Folding. *Trends in Biochemical Sciences*, *41*(1), 62–76. https://doi.org/10.1016/j.tibs.2015.07.009

Heo, K., Jin, H.-E., Kim, H., Lee, J. H., Wang, E., & Lee, S.-W. (2019). Transient self-templating assembly of M13 bacteriophage for enhanced biopiezoelectric devices. *Nano Energy*, *56*, 716–723. https://doi.org/10.1016/j.nanoen.2018.11.084

Heyman, A., Medalsy, I., Bet Or, O., Dgany, O., Gottlieb, M., Porath, D., & Shoseyov, O. (2009). Protein Scaffold Engineering Towards Tunable Surface Attachment. *Angewandte Chemie International Edition*, *48*(49), 9290–9294. https://doi.org/10.1002/anie.200903075

Huang, P-.S., Boyken, S. E., & Baker, D. (2016). The coming of age of *de novo* protein design. *Nature, 537*, 320-327. https://doi.org/10.1038/nature19946

Huber, M. C., Schreiber, A., Wild, W., Benz, K., & Schiller, S. M. (2014). Introducing a combinatorial DNA-toolbox platform constituting defined protein-based biohybrid-materials. *Biomaterials*, *35*(31), 8767–8779. https://doi.org/10.1016/j.biomaterials.2014.06.048

Jang, H. H., Lee, K. O., Chi, Y. H., Jung, B. G., Park, S. K., Park, J. H., … Lee, S. Y. (2004). Two Enzymes in One: Two Yeast Peroxiredoxins Display Oxidative Stress-Dependent Switching from a Peroxidase to a Molecular Chaperone Function. *Cell*, *117*(5), 625–635. https://doi.org/10.1016/j.cell.2004.05.002

Joh, N. H., Wang, T., Bhate, M. P., Acharya, R., Wu, Y., Grabe, M., … DeGrado, W. F. (2014). De novo design of a transmembrane Zn^{2+}-transporting four-helix bundle. *Science, 346*(6216), 1520-1524. DOI: 10.1126/science.1261172

Johnson, J. E., & Speir, J. A. (1997). Quasi-equivalent viruses: a paradigm for protein assemblies. Journal of Molecular Biology, 269(5), 665-675. https://doi.org/10.1006/jmbi.1997.1068

Kehoe, J. W., & Kay, B. K. (2005). Filamentous Phage Display in the New Millennium. *Chemical Reviews*, *105*(11), 4056–4072. https://doi.org/10.1021/cr000261r

Kendall, A., McDonald, M., & Stubbs, G. (2007). Precise determination of the helical repeat of tobacco mosaic virus. *Virology*, *369*(1), 226–227. https://doi.org/10.1016/j.virol.2007.08.013

King, N. P., Bale, J. B., Sheffler, W., McNamara, D. E., Gonen, S., Gonen, T., ... Baker, D. (2014). Accurate design of co-assembling multi-component protein nanomaterials. Nature, 510, 103-108. https://doi.org/10.1038/nature13404

Klug, A. (1999). The tobacco mosaic virus particle: structure and assembly. *Philosophical Transactions of the Royal Society B: Biological Sciences*, *354*(1383), 531-535. doi:10.1098/rstb.1999.0404

Koopmann, R., Cupelli, K., Redecke, L., Nass, K., DePonte , D. P., White, T. A., … Duszenko, M. (2012). In vivo protein crystallization opens new routes in structural biology. *Nature Methods, 9*(3), 259-262. https://doi.org/10.1038/nmeth.1859

Korpi, A., Ma, C., Liu, K., Nonappa, Herrmann, A., Ikkala, O., & Kostiainen, M. A. (2018). Self-Assembly of Electrostatic Cocrystals from Supercharged Fusion Peptides and Protein Cages. *ACS Macro Letters*, *7*(3), 318–323. https://doi.org/10.1021/acsmacrolett.8b00023

Koskela, J. E., Liljeström, V., Lim, J., Simanek, E. E., Ras, R. H. A., Priimagi, A., & Kostiainen, M. A. (2014). Light-Fuelled Transport of Large Dendrimers and Proteins. *Journal of the American Chemical Society*, *136*(19), 6850–6853. https://doi.org/10.1021/ja502623m

Kostiainen, M. A., Ceci, P., Fornara, M., Hiekkataipale, P., Kasyutich, O., Nolte, R. J. M., … van Lierop, J. (2011a). Hierarchical Self-Assembly and Optical Disassembly for Controlled Switching of Magnetoferritin Nanoparticle Magnetism. *ACS Nano*, *5*(8), 6394–6402. https://doi.org/10.1021/nn201571y

Kostiainen, M. A., Hiekkataipale, P., de la Torre, J. Á., Nolte, R. J. M., & Cornelissen, J. J. L. M. (2011b). Electrostatic self-assembly of virus–polymer complexes. *Journal of Materials Chemistry*, *21*(7), 2112–2117. https://doi.org/10.1039/C0JM02592E

Kostiainen, M. A., Hiekkataipale, P., Laiho, A., Lemieux, V., Seitsonen, J., Ruokolainen, J., & Ceci, P. (2013). Electrostatic assembly of binary nanoparticle superlattices using protein cages. *Nature Nanotechnology*, *8*(1), 52–56. https://doi.org/10.1038/nnano.2012.220

Kostiainen, M. A., Kasyutich, O., Cornelissen, J. J. L. M., & Nolte, R. J. M. (2010). Self-assembly and optically triggered disassembly of hierarchical dendron–virus complexes. *Nature Chemistry*, *2*(5), 394–399. https://doi.org/10.1038/nchem.592

Kostiainen, M. A., Pietsch, C., Hoogenboom, R., Nolte, R. J. M., & Cornelissen, J. J. L. M. (2011c). Temperature-Switchable Assembly of Supramolecular Virus-Polymer Complexes. *Advanced Functional Materials*, *21*(11), 2012–2019. https://doi.org/10.1002/adfm.201002597

Künzle, M., Eckert, T., & Beck, T. (2016). Binary Protein Crystals for the Assembly of Inorganic Nanoparticle Superlattices. *Journal of the American Chemical Society*, *138*(39), 12731–12734. https://doi.org/10.1021/jacs.6b07260

Künzle, M., Mangler, J., Lach, M., & Beck, T. (2018). Peptide-directed encapsulation of inorganic nanoparticles into protein containers. *Nanoscale*, *10*(48), 22917–22926. https://doi.org/10.1039/C8NR06236F

Lach, M., Künzle, M., & Beck, T. (2017). Free-Standing Metal Oxide Nanoparticle Superlattices Constructed with Engineered Protein Containers Show in Crystallo Catalytic Activity. *Chemistry - A European Journal*, *23*(69), 17482–17486. https://doi.org/10.1002/chem.201705061

Lavelle, L., Gingery, M., Phillips, M., Gelbart, W. M., Knobler, C. M., Cadena-Nava, R. D., ... Ruiz-Garcia, J. (2009). Phase Diagram of Self-assembled Viral Capsid Protein Polymorphs. Journal of Physical Chemistry B, 113(12), 3813-3819. https://doi.org/10.1021/jp8079765

Lee, J. H., Fan, B., Samdin, T. D., Monteiro, D. A., Desai, M. S., Scheideler, O., … Lee, S.-W. (2017a). Phage-Based Structural Color Sensors and Their Pattern Recognition Sensing System. *ACS Nano*, *11*(4), 3632–3641. https://doi.org/10.1021/acsnano.6b07942

Lee, J. H., Warner, C. M., Jin, H.-E., Barnes, E., Poda, A. R., Perkins, E. J., & Lee, S.-W. (2017b). Production of tunable nanomaterials using hierarchically assembled bacteriophages. *Nature Protocols*, *12*(9), 1999–2013. https://doi.org/10.1038/nprot.2017.085

Lee, L. A., Muhammad, S. M., Nguyen, Q. L., Sitasuwan, P., Horvath, G., & Wang, Q. (2012). Multivalent Ligand Displayed on Plant Virus Induces Rapid Onset of Bone Differentiation. *Molecular Pharmaceutics*, *9*(7), 2121–2125. https://doi.org/10.1021/mp300042t

Lee, S.-W., Wood, B. M., & Belcher, A. M. (2003a). Chiral Smectic C Structures of Virus-Based Films. *Langmuir*, *19*(5), 1592–1598. https://doi.org/10.1021/la026387w

Lee, S.-K., Yun, D. S., & Belcher, A. M. (2006). Cobalt Ion Mediated Self-Assembly of Genetically Engineered Bacteriophage for Biomimetic Co−Pt Hybrid Material. *Biomacromolecules*, *7*(1), 14–17. https://doi.org/10.1021/bm050691x

Lee, S.-W., Lee, S. K., & Belcher, A. M. (2003b). Virus-Based Alignment of Inorganic, Organic, and Biological Nanosized Materials. *Advanced Materials*, *15*(9), 689–692. https://doi.org/10.1002/adma.200304818

Lee, S.-W., Mao, C., Flynn, C. E., & Belcher, A. M. (2002). Ordering of Quantum Dots Using Genetically Engineered Viruses. *Science*, *296*(5569), 892–895. https://doi.org/10.1126/science.1068054

Li, T., Ye, B., Niu, Z., Thompson, P., Seifert, S., Lee, B., & Wang, Q. (2009). Close-Packed Colloidal Assemblies from Icosahedral Plant Virus and Polymer. Chemistry of Materials, 21(6), 1046-1050. https://doi.org/10.1021/cm802922z

Li, T., Winans, R. E., & Lee, B. (2011). Superlattice of Rodlike Virus Particles Formed in Aqueous Solution through Like-Charge Attraction. *Langmuir*, *27*(17), 10929–10937. https://doi.org/10.1021/la202121s

Li, T., Zan, X., Sun, Y., Zuo, X., Li, X., Senesi, A., … Lee, B. (2013a). Self-Assembly of Rodlike Virus to Superlattices. *Langmuir*, *29*(41), 12777–12784. https://doi.org/10.1021/la402933q

Li, T., Zan, X., Winans, R. E., Wang, Q., & Lee, B. (2013b). Biomolecular Assembly of Thermoresponsive Superlattices of the Tobacco Mosaic Virus with Large Tunable Interparticle Distances. *Angewandte Chemie International Edition*, *52*(26), 6638–6642. https://doi.org/10.1002/anie.201209299

Liljeström, V., Mikkilä, J., & Kostiainen, M. A. (2014). Self-assembly and modular functionalization of three-dimensional crystals from oppositely charged proteins. Nature Communications, 5. https://doi.org/10.1038/ncomms5445

Liljeström, V., Ora, A., Hassinen, J., Rekola, H. T., Nonappa, Heilala, M., … Kostiainen, M. A. (2017). Cooperative colloidal self-assembly of metal-protein superlattice wires. *Nature Communications*, *8*(1). https://doi.org/10.1038/s41467-017-00697-z

Liljeström, V., Seitsonen, J., & Kostiainen, M. A. (2015). Electrostatic Self-Assembly of Soft Matter Nanoparticle Cocrystals with Tunable Lattice Parameters. *ACS Nano*, *9*(11), 11278–11285. https://doi.org/10.1021/acsnano.5b04912

Lin, Y., Balizan, E., Lee, L. A., Niu, Z., & Wang, Q. (2010). Self-Assembly of Rodlike Bio-nanoparticles in Capillary Tubes. *Angewandte Chemie*, *122*(5), 880–884. https://doi.org/10.1002/ange.200904993

Liu, K., Chen, D., Marcozzi, A., Zheng, L., Su, J., Pesce, D., … Herrmann, A. (2014). Thermotropic liquid crystals from biomacromolecules. *Proceedings of the National Academy of Sciences*, *111*(52), 18596–18600. https://doi.org/10.1073/pnas.1421257111

Liu, S., Zan, T., Chen, S., Pei, X., Li, H., & Zhang, Z. (2015). Thermoresponsive Chiral to Nonchiral Ordering Transformation in the Nematic Liquid-Crystal Phase of Rodlike Viruses: Turning the Survival Strategy of a Virus into Valuable Material Properties. *Langmuir*, *31*(25), 6995–7005. https://doi.org/10.1021/acs.langmuir.5b01476

Lowther, W. T., & Haynes, A. C. (2011). Reduction of Cysteine Sulfinic Acid in Eukaryotic, Typical 2-Cys Peroxiredoxins by Sulfiredoxin. *Antioxidants & Redox Signaling*, *15*(1), 99–109. https://doi.org/10.1089/ars.2010.3564

Luo, Q., Hou, C., Bai, Y., Wang, R., & Liu, J. (2016). Protein Assembly: Versatile Approaches to Construct Highly Ordered Nanostructures. *Chemical Reviews*, *116*(22), 13571–13632. https://doi.org/10.1021/acs.chemrev.6b00228

Luque, D., de la Escosura, A., Snijder, J. Brasch, M. Burnley, R. J., Koay, M. S. T., ... Caston, J. R. (2014). Self-assembly and characterization of small and monodisperse dye nanospheres in a protein cage. Chemical Science, 5(2), 575-581. https://doi.org/10.1039/C3SC52276H

Lydon, J. (2014). Virus Particle-Based Liquid Crystals. In J. W. Goodby, C. Tschierske, P. Raynes, H. Gleeson, T. Kato, & P. J. Collings (Eds.), *Handbook of Liquid Crystals* (pp. 1–36). Weinheim, Germany: Wiley-VCH Verlag GmbH & Co. KGaA. https://doi.org/10.1002/9783527671403.hlc094

Maity, B., Abe, S., & Ueno, T. (2017). Observation of gold sub-nanocluster nucleation within a crystalline protein cage. *Nature Communications*, *8*, 14820. https://doi.org/10.1038/ncomms14820

Majetich, S. A., Wen, T., & Booth, R. A. (2011). Functional Magnetic Nanoparticle Assemblies: Formation, Collective Behavior, and Future Directions. *ACS Nano*, *5*(8), 6081–6084. https://doi.org/10.1021/nn202883f

Manuguri, S., Webster, K., Yewdall, N. A., An, Y., Venugopal, H., Bhugra, V., … Malmström, J. (2018). Assembly of Protein Stacks With in Situ Synthesized Nanoparticle Cargo. *Nano Letters*, *18*(8), 5138–5145. https://doi.org/10.1021/acs.nanolett.8b02055

McCafferty, J., Griffiths, A. D., Winter, G., & Chiswell, D. J. (1990). Phage antibodies: filamentous phage displaying antibody variable domains. *Nature*, *348*(6301), 552–554. https://doi.org/10.1038/348552a0

McMillan, R. A., Paavola, C. D., Howard, J., Chan, S. L., Zaluzec, N. J., & Trent, J. D. (2002). Ordered nanoparticles arrays formed on engineered chaperonin protein templates. *Nature Materials, 1*, 247-252. https://doi.org/10.1038/nmat775

McMillan, R. A., Howard, J., Zaluzec, N. J., Kagawa, H. K., Mogul, R., Li Y.-F., Paavola, C. D. & Trent, J. D. (2002). A self-assembling protein template for constrained synthesis and patterning of nanoparticle arrays. *Journal of American Chemical Society*, *127*, 2800-28001. https://10.1021/ja043827s

Medalsy, I., Dgany, O., Sowwan, M., Cohen, H., Yukashevska, A., Wolf, S. G., … Porath, D. (2008). SP1 Protein-Based Nanostructures and Arrays. *Nano Letters*, *8*(2), 473–477. https://doi.org/10.1021/nl072455t

Miao, L., Han, J., Zhang, H., Zhao, L., Si, C., Zhang, X., … Liu, J. (2014). Quantum-Dot-Induced Self-Assembly of Cricoid Protein for Light Harvesting. *ACS Nano*, *8*(4), 3743–3751. https://doi.org/10.1021/nn500414u

Mikkilä, J., Anaya-Plaza, E., Liljeström, V., Caston, J. R., Torres, T., de la Escosura, A., & Kostiainen, M. A. (2016). Hierarchical Organization of Organic Dyes and Protein Cages into Photoactive Crystals. *ACS Nano*, *10*(1), 1565–1571. https://doi.org/10.1021/acsnano.5b07167

Mikkilä, J., Rosilo, H., Nummelin, S., Seitsonen, J., Ruokolainen, J., & Kostiainen, M. A. (2013). Janus-Dendrimer-Mediated Formation of Crystalline Virus Assemblies. *ACS Macro Letters*, *2*(8), 720–724. https://doi.org/10.1021/mz400307h

Nelson, N. (2009). Plant photosystem I - the most efficient nano-photochemical machine. Journal of Nanoscience and Nanotechnology, 9(3), 1709-1713. https://doi.org/10.1166/jnn.2009.SI01

Nedoluzhko, A., & Douglas, T. (2001). Ordered association of tobacco mosaic virus in the presence of divalent metal ions. *Journal of Inorganic Biochemistry*, *84*(3–4), 233–240. https://doi.org/10.1016/S0162-0134(01)00174-X

Okuda, M., Suzumoto, Y., & Yamashita, I. (2011). Bioinspired Synthesis of Homogenous Cerium Oxide Nanoparticles and Two- or Three-Dimensional Nanoparticle Arrays Using Protein Supramolecules. *Crystal Growth & Design, 11*(6), 2540-2545. https://doi.org/10.1021/cg200299y

Pallarola, D., Bildering, C. von, Pietrasanta, L. I., Queralto, N., Knoll, W., Battaglini, F., & Azzaroni, O. (2012). Recognition-driven layer-by-layer construction of multiprotein assemblies on surfaces: a biomolecular toolkit for building up chemoresponsive bioelectrochemical interfaces. *Physical Chemistry Chemical Physics*, *14*(31), 11027. https://doi.org/10.1039/c2cp41225j

Perkins, A., Nelson, K. J., Parsonage, D., Poole, L. B., & Karplus, P. A. (2015). Peroxiredoxins: guardians against oxidative stress and modulators of peroxide signaling. *Trends in Biochemical Sciences*, *40*(8), 435–445. https://doi.org/10.1016/j.tibs.2015.05.001

Petrenko V. A., & Vodyanoy V. J. (2003). Phage display for detection of biological threat agents. *Journal of Microbiological Methods, 53*(2), 253-262. https://doi.org/10.1016/S0167-7012(03)00029-0

Phillips, A. J., Littlejohn, J., Yewdall, N. A., Zhu, T., Valéry, C., Pearce, F. G., … Gerrard, J. A. (2014). Peroxiredoxin is a Versatile Self-Assembling Tecton for Protein Nanotechnology. *Biomacromolecules*, *15*(5), 1871–1881. https://doi.org/10.1021/bm500261u

Prinsen, P., van der Schoot, P., Gelbart, W. M., & Knobler, C. M. (2010). Multishell Structures of Virus Coat Proteins. *The Journal of Physical Chemistry B*, *114*(16), 5522–5533. https://doi.org/10.1021/jp911040z

Qin, X., Suga, M., Kuang, T., & Shen, J.-R. (2015). Structural basis for energy transfer pathways in the plant PSI-LHCI supercomplex. *Science, 348*(6238), 989-995. http://doi.org/10.1126/science.aab0214

Rhee, S. G., Chae, H. Z., & Kim, K. (2005). Peroxiredoxins: A historical overview and speculative preview of novel mechanisms and emerging concepts in cell signaling. *Free Radical Biology and Medicine*, *38*(12), 1543–1552. https://doi.org/10.1016/j.freeradbiomed.2005.02.026

Riekel, C., Burghammer, M., Snigirev, I., & Rosenthal, M. (2018). Microstructural metrology of tobacco mosaic virus nanorods during radial compression and heating. *Soft Matter*, *14*(2), 194–204. https://doi.org/10.1039/C7SM01332A

de Ruiter, M. V., Putri, R. M., & Cornelissen, J. J. L. M. (2018). CCMV-Based enzymatic nanoreactors. In: Wege C., Lomonossof G. (eds) Virus- derived nanoparticles for advanced Technologies. methos in Molecular Biology, vol 1776, pp 237-247. Humana Press, New York, NY. https://doi.org/10.1007/978-1-4939-7808-3_16

Salgado, E. N., Lewis, R. A., Mossin, S., Rheingold, A. L., & Tezcan, F. A. (2009). Control of Protein Oligomerization Symmetry by Metal Coordination: C_2 and C_3 Symmetrical Assemblies through Cu^{II} and Ni^{II} Coordination. *Inorganic Chemistry*, *48*(7), 2726–2728. https://doi.org/10.1021/ic9001237

Sanchez, C., Arribart, H., & Giraud Guille, M. M. (2005). Biomimetism and bioinspiration as tools for the design of innovative materials and systems. *Nature Materials*, *4*(4), 277–288. https://doi.org/10.1038/nmat1339

Schenk, A. S., Eiben, S., Goll, M., Reith, L., Kulak, A. N., Meldrum, F. C., … Ludwigs, S. (2017). Virus-directed formation of electrocatalytically active nanoparticle-based Co_3O_4 tubes. *Nanoscale*, *9*(19), 6334–6345. https://doi.org/10.1039/C7NR00508C

Schlick, T. L., Ding, Z., Kovacs, E. W., & Francis, M. B. (2005). Dual-Surface Modification of the Tobacco Mosaic Virus. *Journal of the American Chemical Society*, *127*(11), 3718–3723. https://doi.org/10.1021/ja046239n

Schnirman, A. A., Zahavi, E., Yeger, H., Rosenfeld, R., Benhar, I., Reiter, Y., & Sivan U. (2006). Antibody molecules discriminate between crystalline facets of a gallium arsenide semiconductor. *Nano Letters, 6*(9), 1870-1874. https://doi.org/10.1021/nl060763

Schreiber, A., Huber, M. C., Cölfen, H., & Schiller, S. M. (2015). Molecular protein adaptor with genetically encoded interaction sites guiding the hierarchical assembly of plasmonically active nanoparticle architectures. *Nature Communications*, *6*, 6705. https://doi.org/10.1038/ncomms7705

Scott, J., & Smith, G. (1990). Searching for peptide ligands with an epitope library. *Science*, *249*(4967), 386–390. https://doi.org/10.1126/science.1696028

Sendai, T., Biswas, S., & Aida, T. (2013). Photoreconfigurable Supramolecular Nanotube. *Journal of the American Chemical Society*, *135*(31), 11509–11512. https://doi.org/10.1021/ja4060146

Setaro, F., Brasch, M., Hahn, U., Koay, M. S. T., Cornelissen, J. J. L. M., de la Escosura, A., & Torres, T. (2015). Generation-Dependent Templated Self-Assembly of Biohybrid Protein Nanoparticles around Photosensitizer Dendrimers. *Nano Letters*, *15*(2), 1245–1251. https://doi.org/10.1021/nl5044055

Sikkema, F. D., Comellas-Aragones, M., Fokkink, R. G., Verduin, B. J. M., Cornelissen, J. L. M., & Nolte, R. J. M. (2007). Monodisperse polymer-virus hybrid nanoparticles. *Organic and Biomolecular Chemistry, 5*(1), 54-57. https://doi.org/10.1039/B613890J

Sim, S., Miyajima, D., Niwa, T., Taguchi, H., & Aida, T. (2015). Tailoring Micrometer-Long High-Integrity 1D Array of Superparamagnetic Nanoparticles in a Nanotubular Protein Jacket and

Its Lateral Magnetic Assembling Behavior. *Journal of the American Chemical Society*, *137*(14), 4658–4661. https://doi.org/10.1021/jacs.5b02144

Sim, S., Niwa, T., Taguchi, H., & Aida, T. (2016). Supramolecular Nanotube of Chaperonin GroEL: Length Control for Cellular Uptake Using Single-Ring GroEL Mutant as End-Capper. *Journal of the American Chemical Society*, *138*(35), 11152–11155. https://doi.org/10.1021/jacs.6b07925

Smith, G. P., & Petrenko, V. A. (1997). Phage Display. *Chemical Reviews*, *97*(2), 391–410. https://doi.org/10.1021/cr960065d

Sontz, P. A., Bailey, J. B., Ahn, S., & Tezcan, F. A. (2015). A Metal Organic Framework with Spherical Protein Nodes: Rational Chemical Design of 3D Protein Crystals. *Journal of the American Chemical Society*, *137*(36), 11598–11601. https://doi.org/10.1021/jacs.5b07463

Sontz, P. A., Song, W. J., & Tezcan, F. A. (2014). Interfacial metal coordination in engineered protein and peptide assemblies. *Current Opinion in Chemical Biology*, *19*, 42–49. https://doi.org/10.1016/j.cbpa.2013.12.013

Speir, J. A., Munshi, S., Wang, G. J., Baker, T. S., & Johnson, J. E. (1995). Structures of the native and swollen forms of cowpea chlorotic mottle virus determined by X-ray crystallography and cryo-electron microscopy. *Structure, 3*(1), 63-78. https://doi.org/10.1016/S0969-2126(01)00135-6

Sun, H., Miao, L., Li, J., Fu, S., An, G., Si, C., … Liu, J. (2015). Self-Assembly of Cricoid Proteins Induced by “Soft Nanoparticles”: An Approach To Design Multienzyme-Cooperative Antioxidative Systems. *ACS Nano*, *9*(5), 5461–5469. https://doi.org/10.1021/acsnano.5b01311

Sun, H., Zhang, X., Miao, L., Zhao, L., Luo, Q., Xu, J., & Liu, J. (2016). Micelle-Induced Self-Assembling Protein Nanowires: Versatile Supramolecular Scaffolds for Designing the Light-Harvesting System. *ACS Nano*, *10*(1), 421–428. https://doi.org/10.1021/acsnano.5b05213

Sun, J., DuFort, C., Daniel, M.-C., Murali, A., Chen, C., Gopinath, K., … Dragnea, B. (2007). Core-controlled polymorphism in virus-like particles. *Proceedings of the National Academy of Sciences*, *104*(4), 1354–1359. https://doi.org/10.1073/pnas.0610542104

Szentivanyi, A., Assmann, U., Schuster, R., & Glasmacher, B. (2009). Production of biohybrid protein/PEO scaffolds by electrospinning. *Materialwissenschaft Und Werkstofftechnik*, *40*(1–2), 65–72. https://doi.org/10.1002/mawe.200800376

Tatur, J., Hagen, W. R., & Matias, P. M. (2007). Crystal structure of the ferritin from the hyperthermophilic archaeal anaerobe Pyrococcus furiosus. *JBIC Journal of Biological Inorganic Chemistry*, *12*(5), 615–630. https://doi.org/10.1007/s00775-007-0212-3

Toksoz, S., Acar, H., & Guler, M. O. (2010). Self-assembled one-dimensional soft nanostructures. *Soft Matter*, *6*(23), 5839. https://doi.org/10.1039/c0sm00121j

Uchida, M., McCoy, K., Fukuto, M., Yang, L., Yoshimura, H., Miettinen, H. M., … Douglas, T. (2018). Modular Self-Assembly of Protein Cage Lattices for Multistep Catalysis. *ACS Nano*, *12*(2), 942–953. https://doi.org/10.1021/acsnano.7b06049

Ueno, T. (2013). Porous Protein Crystals as Reaction Vessels. *Chemistry - A European Journal*, *19*(28), 9096–9102. https://doi.org/10.1002/chem.201300250

Ueno, T., Suzuki, M., Goto, T., Matsumoto, T., Nagayama, K., & Watanabe, Y. (2004). Size-Selective Olefin Hydrogenation by a Pd Nanocluster Provided in an Apo-Ferritin Cage. *Angewandte Chemie International Edition*, *43*(19), 2527–2530. https://doi.org/10.1002/anie.200353436

Välimäki, S., Mikkilä, J., Liljeström, V., Rosilo, H., Ora, A., & Kostiainen, M. (2015). Hierarchically Ordered Supramolecular Protein-Polymer Composites with Thermoresponsive Properties. *International Journal of Molecular Sciences*, *16*(5), 10201–10213. https://doi.org/10.3390/ijms160510201

van Wezenbeek, P. M. G. F., Hulsebos, T. J. M., & Schoenmakers, J. G. G. (1980). Nucleotide sequence of the filamentous bacteriophage M13 DNA genome: comparison with phage fd. *Gene*, *11*(1), 129–148. https://doi.org/10.1016/0378-1119(80)90093-1

Vilenchik, L. Z., Griffith, J. P., St. Clair, N., Navia, M. A., & Margolin, A. L. (1998). Protein Crystals as Novel Microporous Materials. *Journal of the American Chemical Society*, *120*(18), 4290–4294. https://doi.org/10.1021/ja973449+

Wang, W.-X., Dgany, O., Dym, O., Altman, A., Shoseyov, O., & Almog, O. (2003). Crystallization and preliminary X-ray crystallographic analysis of SP1, a novel chaperone-like protein. *Acta Crystallographica Section D: Biological Crystallography*, *59*(3), 512–514. https://doi.org/10.1107/S0907444902022618

Wang, W.-X., Dgany, O., Wolf, S. G., Levy, I., Algom, R., Pouny, Y., … Shoseyov, O. (2006). Aspen SP1, an exceptional thermal, protease and detergent-resistant self-assembled nano-particle. *Biotechnology and Bioengineering*, *95*(1), 161–168. https://doi.org/10.1002/bit.21010

Wang, W.-X., Pelah, D., Alergand, T., Shoseyov, O., & Altman, A. (2002). Characterization of SP1, a Stress-Responsive, Boiling-Soluble, Homo-Oligomeric Protein from Aspen. *Plant Physiology*, *130*(2), 865–875. https://doi.org/10.1104/pp.002436

Wen, A. M., & Steinmetz, N. (2016). Design of virus-based nanomaterials for medicine, biotechnology, and energy. *Chemical Society Reviews, 45*, 4074–4126. https://doi.org/10.1039/C5CS00287G

Whaley, S. R., English, D. S., Hu, E. L., Barbara, P. F., & Belcher, A. M. (2000). Selection of peptides with semiconductor binding specificity for directed nanocrystal assembly. *Nature*, *405*, 665–668.

Whitesides, G. M., & Boncheva, M. (2002). Beyond molecules: Self-assembly of mesoscopic and macroscopic components. *Proceedings of the National Academy of Sciences*, *99*(8), 4769–4774. https://doi.org/10.1073/pnas.082065899

Wu, Y., Jiang, Z., Zan, X., Lin, Y., & Wang, Q. (2017). Shear flow induced long-range ordering of rod-like viral nanoparticles within hydrogel. *Colloids and Surfaces B: Biointerfaces*, *158*, 620–626. https://doi.org/10.1016/j.colsurfb.2017.07.039

Xu, Z., Horwich, A. L., & Sigler, P. B. (1997). The crystal structure of the asymmetric GroEL–GroES–$(ADP)_7$ chaperonin complex. *Nature*, *388*(6644), 741–750. https://doi.org/10.1038/41944

Yang, J., Yoon, M. -C., Yoo, H., Kim, P., & Kim, D. (2012). Excitation energy transfer in multiporphyrin arrays with cyclic architectures: towards artificial light-harvesting antenna complexes. *Chemical Society Reviews, 41*,(12), 4808-4826. http://doi.org/10.1039/C2CS35022J

Yang, S. H., Chung, W.-J., McFarland, S., & Lee, S.-W. (2013). Assembly of Bacteriophage into Functional Materials: Assembly of Bacteriophage into Functional Materials. *The Chemical Record*, *13*(1), 43–59. https://doi.org/10.1002/tcr.201200012

Yewdall, N. A., Venugopal, H., Desfosses, A., Abrishami, V., Yosaatmadja, Y., Hampton, M. B., … Radjainia, M. (2016). Structures of Human Peroxiredoxin 3 Suggest Self-Chaperoning Assembly that Maintains Catalytic State. *Structure*, *24*(7), 1120–1129. https://doi.org/10.1016/j.str.2016.04.013

Zan, X., Feng, S., Balizan, E., Lin, Y., & Wang, Q. (2013). Facile Method for Large Scale Alignment of One Dimensional Nanoparticles and Control over Myoblast Orientation and Differentiation. *ACS Nano*, *7*(10), 8385–8396. https://doi.org/10.1021/nn403908k

Zhang, J., Wang, X., Zhou, K., Chen, G., & Wang, Q. (2018). Self-Assembly of Protein Crystals with Different Crystal Structures Using Tobacco Mosaic Virus Coat Protein as a Building Block. *ACS Nano*, *12*(2), 1673–1679. https://doi.org/10.1021/acsnano.7b08316

Zhang, S. (2003). Fabrication of novel biomaterials through molecular self-assembly. *Nature Biotechnology*, *21*(10), 1171–1178. https://doi.org/10.1038/nbt874

Zhao, L., Zou, H., Zhang, H., Sun, H., Wang, T., Pan, T., … Liu, J. (2017). Enzyme-Triggered Defined Protein Nanoarrays: Efficient Light-Harvesting Systems to Mimic Chloroplasts. *ACS Nano*, *11*(1), 938–945. https://doi.org/10.1021/acsnano.6b07527